J. Fluid Mech. (1995), *vol.* 300, *pp.* 117–147

Stability of spatially developing boundary layers in pressure gradients

By RAMA GOVINDARAJAN[1] AND R. NARASIMHA[2]

[1] Computational and Theoretical Fluid Dynamics Division, National Aerospace Laboratories, Bangalore 560 017, India

[2] Jawaharlal Nehru Centre for Advanced Scientific Research and Department of Aerospace Engineering, Indian Institute of Science, Bangalore 560 012, India

(Received 19 April 1994 and in revised form 20 May 1995)

A new formulation of the stability of boundary-layer flows in pressure gradients is presented, taking into account the spatial development of the flow and utilizing a special coordinate transformation. The formulation assumes that disturbance wavelength and eigenfunction vary downstream no more rapidly than the boundary-layer thickness, and includes all terms nominally of order R^{-1} in the boundary-layer Reynolds number R. In Blasius flow, the present approach is consistent with that of Bertolotti *et al.* (1992) to $O(R^{-1})$ but simpler (i.e. has fewer terms), and may best be seen as providing a parametric differential equation which can be solved without having to march in space. The computed neutral boundaries depend strongly on distance from the surface, but the one corresponding to the inner maximum of the streamwise velocity perturbation happens to be close to the parallel flow (Orr–Sommerfeld) boundary. For this quantity, solutions for the Falkner–Skan flows show the effects of spatial growth to be striking only in the presence of strong adverse pressure gradients. As a rational analysis to $O(R^{-1})$ demands inclusion of higher-order corrections on the mean flow, an illustrative calculation of one such correction, due to the displacement effect of the boundary layer, is made, and shown to have a significant destabilizing influence on the stability boundary in strong adverse pressure gradients. The effect of non-parallelism on the growth of relatively high frequencies can be significant at low Reynolds numbers, but is marginal in other cases. As an extension of the present approach, a method of dealing with non-similar flows is also presented and illustrated.

However, inherent in the transformation underlying the present approach is a lower-order non-parallel theory, which is obtained by dropping all terms of nominal order R^{-1} except those required for obtaining the lowest-order solution in the critical and wall layers. It is shown that a reduced Orr–Sommerfeld equation (in transformed coordinates) already contains the major effects of non-parallelism.

1. Introduction

The investigation of the hydrodynamic stability of the laminar boundary layer has had a long and somewhat controversial history. The evolution of small periodic disturbances imposed on a *parallel* flow is generally investigated through the Orr–Sommerfeld equation, which has been extensively treated in Drazin & Reid (1981). Solutions of this equation, indicating the stability boundary for the laminar boundary layer on a flat plate, were first obtained by Tollmien in 1929; the predicted unstable waves were eventually observed in the careful experiments of Schubauer & Skramstad (1948). Although the qualitative predictions of the theory leading to the TS

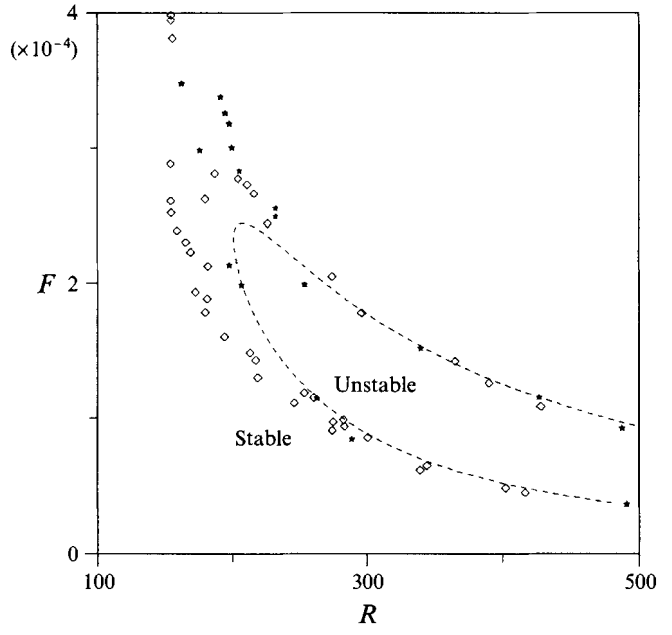

FIGURE 1. Comparison of parallel flow theory (----) with experiment: *, Schubauer & Skramstad (1948); ◇, Ross *et al.* (1970).

waves (as they are called – after Tollmien and Schlichting/Schubauer) have thus been confirmed, there is still disagreement among different workers on the precise quantitative parameters describing this instability. To see why this is so, we first present the results from classical Orr–Sommerfeld theory. Figure 1 shows the stability boundary computed by Gaster (1974) in the plane of the non-dimensional frequency parameter $F = \omega_d \nu / U^2$ and the Reynolds number $R = U\theta/\nu$, where ω_d is the dimensional frequency of the disturbance, U is the (dimensional) free-stream velocity, θ is the (dimensional) momentum thickness of the boundary layer and ν is the kinematic viscosity of the fluid.

A crucial assumption in such calculations of the stability boundary based on the Orr–Sommerfeld equation is that, although both mean flow and the Reynolds number R vary with downstream distance x (R increases like $x^{1/2}$ in this case), the flow may be considered locally parallel, i.e. mean flow variations in x may be ignored. The Orr–Sommerfeld equation is therefore an ordinary differential equation in the normal coordinate y_d whose solutions at any given station x_d give the band of unstable frequencies in a flow which extends to $\pm\infty$ in x_d with no variation. This is clearly an approximation at best; figure 1 shows a comparison of this Orr–Sommerfeld theory with measurements, from which it can be seen that there are discrepancies, especially at low Reynolds numbers. Several workers have investigated the stability of non-parallel flows in the expectation that this discrepancy may be explained wholly or in part as due to flow non-parallelism. Potentially the most important consequence of including non-parallel effects would appear to be that the simplification to an ordinary differential equation could in general be lost. However, the fact that streamwise derivatives of mean quantities are only $O(R^{-1})$ simplifies the formulation of the non-parallel problem, and has been exploited in some way by most workers.

Apart from the common feature of assuming slow variations in x, the non-parallel problem has been tackled in different ways by different workers and the results are not

always in agreement with each other. The different approaches taken may broadly be categorized as follows: (*a*) modified Orr–Sommerfeld equation (Barry & Ross 1970; Bertolotti, Herbert & Spalart 1992; Sen 1993; and the present work); (*b*) obtaining non-parallel effects by a perturbation of the parallel solution (Bouthier 1972, 1973; Gaster 1974); (*c*) method of multiple scales (Ling & Reynolds 1973; Saric & Nayfeh 1975); (*d*) triple-deck asymptotic expansions (Smith 1979); and (*e*) direct simulation (Fasel & Konzelmann 1990; Bertolotti *et al.* 1992).

Barry & Ross (1970) derived a modified Orr–Sommerfeld equation for the flow over a flat plate where they included the effect of the normal component of the mean velocity which arises due to boundary-layer growth. They neglected any possible streamwise variation in wavenumber and also assumed that the disturbance eigenfunction depends only on distance from the surface non-dimensionalized by a length scale that does not vary streamwise. Bouthier (1972, 1973) included non-parallel effects by considering a perturbation of the Orr–Sommerfeld problem where the Orr–Sommerfeld eigenfunction ϕ is corrected by an x-dependent amplitude as well as a higher-order term ϕ_1. The wavenumber too depends on the streamwise coordinate. Bouthier made the important point that stability depends on the flow quantity being considered (e.g. disturbance kinetic energy, streamwise disturbance velocity, etc.) as well as on the distance from the wall. Ling & Reynolds (1973) derived a modified Orr–Sommerfeld equation where they neglected the streamwise variation of the boundary-layer thickness. Their computed stability boundary for Blasius flow did not differ significantly from the Orr–Sommerfeld boundary. Following the approach of Barry & Ross, Wazzan, Taghavi & Keltner (1974) computed the stability of Falkner–Skan flows. Gaster's (1974) approach was similar to that of Bouthier: the basic assumption was that the disturbances in developing flow could be described in terms of local eigenfunctions with x-dependent amplitudes by means of a perturbation of the Orr–Sommerfeld problem. This approach accounts for all effects of order up to R^{-1}. Gaster noted that the 'neutral stability' boundary measured in an experiment will depend on the path traversed by the measuring probe. He computed stability boundaries by following different paths and compared these with the appropriate experiments. His non-parallel computations show instability at a marginally lower Reynolds number as well as up to a slightly higher frequency than the parallel analysis, but do not entirely remove the discrepancies compared to experiment. His results have provided a standard of comparison for all later work, and are supported by several recent studies, e.g. Fasel & Konzelmann (1990), Bertolotti *et al.* (1992) and the present results.

Saric & Nayfeh (1975) performed a spatial stability analysis on slightly non-parallel flows by the method of multiple scales and computed stability boundaries for Falkner–Skan profiles. In the case of a flat plate, their results matched much better with experiment than Gaster's. However, this agreement was fortuitous (see Drazin & Reid 1981) since they had neglected the streamwise variation in the shape of the disturbance velocity profile. When they accounted for this term in their method, they obtained results in agreement with Gaster's. Smith (1979) considered an asymptotic expansion at large Reynolds numbers and used the triple-deck structure of the disturbances at the lower branch of the neutral stability curve to obtain a correction in the coefficient of $R^{-3/4}$ in the expansion for the neutrally stable frequency. This approach may be followed for the upper branch too. This method is strictly valid only for very large Reynolds numbers and cannot be used to compute the critical Reynolds number accurately. Fasel & Konzelmann (1990) solved the complete Navier–Stokes equations numerically to obtain non-parallel effects in the stability of a Blasius boundary layer. Their results were in good agreement with Gaster's. Bertolotti *et al.* (1992) derived a

'parabolic stability equation' over a flat plate assuming slow variations in the streamwise direction, which they solved by space marching (and locally to obtain initial conditions for the marching procedure). These authors also performed stability studies by direct numerical simulation and found that the results matched those of the parabolic stability equation. Their results, as mentioned before, agree with Gaster's. They report that the computational time required for the local procedure is an order of magnitude greater than that for the marching procedure. Sen (1993) argued that the streamwise derivative of the dimensional wavenumber ($\mathrm{d}\alpha_d/\mathrm{d}x_d$) is negligible while the streamwise derivative of the eigenfunction ($\partial\phi/\partial x_d$), being orthogonal to the eigenfunction ϕ outside the boundary layer, does not alter the results significantly. He used a constant length scale δ_0^* for non-dimensionalizing the disturbance stream function. However, at some stage in the investigation δ_0^* was taken to be numerically equal to the local displacement thickness δ^*. His results agree better with experiment than those of other workers. In work currently underway, M. Thomas & P. K. Sen have incorporated the effects of the x-dependence of the wavenumber and the eigenfunction into Sen's modified equation which still uses the same concept of a locally constant δ_0^*.

The situation (at least till very recently, see below) has therefore been that many of the theoretical approaches provide results in broad agreement among themselves, but not with the experimental results available at low Reynolds numbers. The theory of Sen is an exception, but agreement with experiment is not as simple an issue as it appears at first sight. Among other reasons (discussed at length by Saric 1990) is the sensitivity of experimental results to (i) the track along which the probe is traversed to measure amplification and (ii) the shape and extent of the leading edge of the plate on which the experiment is conducted. The strong influence of the latter has been highlighted in the recent experiments of Klingmann *et al.* (1993), whose results are in good agreement with Gaster's computed results. These workers conclude that the major reason for the departure of their results from earlier experimental work is that in the latter the external velocity was not maintained constant in the vicinity of the leading edge. Klingmann *et al.* ensure a zero pressure gradient in this region by deflecting a tail flap attached to the experimental flat plate; with the flap horizontal, they obtain a neutral stability curve close to those of Schubauer & Skramstad and Ross *et al.* (1970).

It is therefore of value to put the theory of non-parallel flows on a stronger foundation.

In applications boundary layers are often subject to the influence of pressure gradients, not always mild. However, no satisfactory theory of the stability of such flows, taking account of non-parallelism, is available. As a first step in this direction, we study here the stability of spatially developing Falkner–Skan flows. The purpose is to derive and solve a stability equation correct to order R^{-1}. The local free-stream velocity and momentum thickness are used to non-dimensionalize the perturbation equations; this is equivalent to making a coordinate transformation to the similarity variables governing Falkner–Skan flows. This procedure simplifies the ordering of terms and the elimination of all those above a required order; furthermore the Falkner–Skan equation for the mean flow emerges naturally in this formulation. This representation also lends itself to a natural extension to non-similar flows. The disturbance eigenfunction and the wavenumber are assumed to be slowly varying functions of the streamwise distance x, i.e. their derivatives with respect to x are assumed to be $O(R^{-1})$; the second derivatives, being $o(R^{-1})$, are negligible. The resulting equation is a 'degenerate' partial differential equation, i.e. it contains x-

derivatives of the wavenumber as well as the disturbance eigenfunction which at any x-location are a number and a function of y alone respectively, so it can be treated as a parametric differential equation up to the order considered. The method for obtaining the x-derivative terms is described in §3. The present equation contains the Orr–Sommerfeld equation but does not reduce to it in any rational approximation; the lowest-order rational approximation is a 'reduced' Orr–Sommerfeld equation in transformed variables, discussed in §8. For zero pressure gradient, the present results support the non-parallel analysis of Gaster (1974) and do not agree much better with earlier experimental results than the parallel analysis, but it is shown that in the presence of adverse pressure gradients the results of a stability analysis which accounts for the growth of the boundary layer depart significantly at low Reynolds numbers from parallel flow results.

The present formulation and the method of solution are described in §§2 and 3 respectively; a detailed comparison of the present formulation with earlier work is given in Appendix A. The results for Blasius flow are given in §4 while §5 discusses the results for Falkner–Skan flows. The implications of the non-parallel analysis for the e^nmethodology for transition prediction are discussed in §6. The extension to arbitrary pressure gradients is described in §7. Section 8 contains a description of the lowest-order theory mentioned above. A concluding discussion is presented in §9.

2. Formulation for non-parallel flows

2.1. *The equations*

In the classical linear stability analysis of the flow over a flat plate (described for example in Drazin & Reid 1981), the disturbance is broken up into normal modes of the form

$$\hat{\phi} = \phi(y)\, \mathrm{e}^{\mathrm{i}(\alpha x - \omega t)},$$

where α and ω are the wavenumber and frequency of the disturbance respectively. Only two-dimensional disturbances are considered since, for a two-dimensional mean flow, they become unstable at a lower Reynolds number than three-dimensional disturbances (Squire's theorem). Since the disturbances are assumed small, their products may be neglected. If it is further assumed that the boundary layer is locally parallel, i.e. does not grow with x (so $\partial/\partial x = 0$ and the normal velocity is zero), ϕ satisfies the Orr–Sommerfeld equation

$$\{\mathrm{OS}\}\,\phi \equiv \left[\mathrm{i}(\omega - \alpha\Phi')(\mathrm{D}^2 - \alpha^2) + \mathrm{i}\alpha\Phi''' + \frac{1}{R}(\mathrm{D}^4 - 2\alpha^2\mathrm{D}^2 + \alpha^4)\right]\phi = 0 \qquad (1)$$

which defines the Orr–Sommerfeld operator $\{\mathrm{OS}\}$. Equation (1) has been non-dimensionalized using the free-stream velocity U and a boundary-layer thickness (in what follows the momentum thickness θ) as scales; R is the Reynolds number based on the same scales,

$$\mathrm{D}^k \equiv \frac{\mathrm{d}^k}{\mathrm{d}y^k}, \quad k = 1, 2, \ldots,$$

and primes on the mean streamfunction $\Phi(y)$ denote differentiation with respect to y. In spatial stability analysis, $\alpha = \alpha_r + \mathrm{i}\alpha_i$ is taken to be complex and ω to be real, the boundary layer being unstable to a given disturbance if α_i is negative.

To see how the assumption of parallelism in the Orr–Sommerfeld equation may be

relaxed, we return to the incompressible Navier–Stokes equations in two-dimensional flow, which may be written in terms of the streamfunction ψ_d as

$$\frac{\partial}{\partial t_d}\nabla_d^2\psi_d+\frac{\partial\psi_d}{\partial y_d}\frac{\partial}{\partial x_d}\nabla_d^2\psi_d-\frac{\partial\psi_d}{\partial x_d}\frac{\partial}{\partial y_d}\nabla_d^2\psi_d-\nu\nabla_d^4\psi_d=0, \tag{2}$$

where the subscript d indicates a dimensional quantity. The streamfunction may be expressed as the sum of a steady mean and a time-dependent perturbation,

$$\psi_d(x_d,y_d,t)=\Phi_d(x_d,y_d)+\hat{\phi}_d(x_d,y_d,t_d).$$

First the following non-dimensionalization is used:

$$\left.\begin{aligned}&\psi_d=U(x_d)\,\theta(x_d)\,\psi,\quad \mathrm{d}x=\frac{\mathrm{d}x_d}{\theta},\quad y=\frac{y_d}{\theta},\quad \alpha=\alpha_d\theta,\quad \omega=\frac{\omega_d\theta}{U},\\&\psi=\Phi(y)+\phi(x,y)\exp\left(\mathrm{i}\left[\int\alpha(x)\,\mathrm{d}x-\omega_d t_d\right]\right).\end{aligned}\right\} \tag{3}$$

It can be seen that the non-dimensionalization adopted, especially for the streamwise distance x, represents a departure from all earlier work; although not essential, the above approach makes it easier to establish connections with the Orr–Sommerfeld equation, to which we shall return in §8. It must be noted that as θ is permitted to be a function of x, the variable y, here and in all subsequent equations, is proportional to the variable usually denoted as η in similarity solutions of the boundary-layer equations. For a Falkner–Skan profile, $U\sim x_d^m$ where m is a constant. Therefore

$$x=\frac{2x_d}{(1+m)\,\theta}=\frac{R}{p},\quad \frac{\mathrm{d}\theta}{\mathrm{d}x_d}=\frac{q}{R},\quad \frac{\mathrm{d}(U\theta)}{\mathrm{d}x_d}=\frac{Up}{R}, \tag{4}$$

where p and q are constants given by

$$p=\theta^{*2},\quad q=\theta^{*2}\frac{1-m}{1+m},\quad \theta^*\equiv\left(\frac{(1+m)\,U}{2\nu x_d}\right)^{1/2}\int_0^\infty\Phi'(1-\Phi')\,\mathrm{d}y_d.$$

We note that $\mathrm{d}\theta/\mathrm{d}x_d=O(R^{-1})$, and assume that α and ϕ cannot vary faster (in x) than θ, i.e. that their first derivatives with respect to x are at most of order R^{-1}, and that their second derivatives are $o(R^{-1})$ and can therefore be neglected. On substituting this in (2) it is seen that the mean flow equation is given by

$$\Phi^{\mathrm{iv}}+p\Phi\Phi'''+(2q-p)\,\Phi'\Phi''=0, \tag{5}$$

which is the Falkner–Skan equation differentiated once with respect to y. Unlike in the traditional Orr–Sommerfeld approach, the correct mean flow equation emerges naturally here. The disturbance streamfunction is given by

$$\{\mathrm{NP}\}\,\phi=0,$$

where the operator, including all terms nominally of $O(R^{-1})$, is

$$\begin{aligned}\{\mathrm{NP}\}\equiv\Bigg\{&\mathrm{i}(\omega-\alpha\Phi')\,\mathrm{D}^2+\mathrm{i}\alpha[-\alpha(\omega-\alpha\Phi')+\Phi'']+\frac{1}{R}\Big(\mathrm{D}^4+p\Phi\,\mathrm{D}^3\\&+[-2\alpha^2+(2q-p)\,\Phi']\,\mathrm{D}^2+[2yq\alpha(\omega-\alpha\Phi')-p\alpha^2\Phi+(2q-p)\,\Phi'']\,\mathrm{D}\\&+[\alpha^4+(q-2p)\,\alpha\omega+p\Phi'''+3(p-q)\,\alpha^2\Phi']+(-\omega+3\alpha\Phi')\,R\alpha'\\&+[\Phi'''+3\alpha^2\Phi'-2\alpha\omega-\Phi'\mathrm{D}^2]\,R\frac{\partial}{\partial x}\Big)\Bigg\}.\end{aligned} \tag{6}$$

Here, terms of $O(y/R^2)$ have been neglected, hence the above equation is valid as long as $y\sim o(R)$. Since α'' and $\partial^2\phi/\partial x^2$ are both negligible, at a given Reynolds number α' and $\partial\phi/\partial x$ are independent of x (α' is a number and $\partial\phi/\partial x$ is a function only of y). It

therefore follows that the above partial differential equation can be treated like an ordinary differential equation in y for any prescribed value of R, which plays the role of a parameter just as in the Orr–Sommerfeld equation: indeed (6) is best considered as a parametric differential equation. However α' and $\partial\phi/\partial x$ are not known, and may be computed for instance by the iterative procedure described in §3.

2.2. *Boundary conditions*

The boundary conditions are

$$\phi = \mathrm{D}\phi = 0 \quad \text{at} \quad y = 0, \tag{7}$$

$$\phi \to 0, \quad \mathrm{D}\phi \to 0 \quad \text{as} \quad y \to \infty. \tag{8}$$

It is shown in Appendix B that at large y the eigenfunction decays as

$$\phi = f(x)\exp\left[-\alpha y + \mathrm{i}\frac{p + Rf'/f}{R}y + \mathrm{i}\frac{q\alpha - R\alpha'}{2R}y^2\right]. \tag{9}$$

Here, $f(x)$ is fixed by the normalization chosen for ϕ, which is described later in this section. Sen (1993) assumed a form similar to the one obtained above for his modified Orr–Sommerfeld equation. In order that ϕ decay at large y the real part of the exponent in (9) must be negative, i.e. we must have

$$2[\alpha_r + \mathrm{Im}\,(f'/f)]\,y + (q\alpha_i/R - \mathrm{d}\alpha_i/\mathrm{d}x)\,y^2 > 0. \tag{10}$$

Since $(f'/f) \sim O(R^{-1})$, we have $\alpha_r \gg \mathrm{Im}\,(f'/f)$, hence the coefficient of y in the above inequality is positive. Close to the neutral stability curve α_i is small, so

$$\frac{\mathrm{d}\alpha_i}{\mathrm{d}x} = p\frac{\mathrm{d}\alpha_i}{\mathrm{d}R} \gg \frac{q\alpha_i}{R}$$

and the first coefficient of y^2 in (10) can be neglected. At the lower branch of the neutral stability curve $\mathrm{d}\alpha_i/\mathrm{d}x < 0$, so ϕ always decays with increasing y. At the upper branch, however, $\mathrm{d}\alpha_i/\mathrm{d}x > 0$, but ϕ decays as y increases till $y \sim O(\alpha_r/\alpha_i)$. Since α_i is very close to 0 the real part of the exponent is negative up to a very large value of y, where the analysis is anyway not valid since (6) has been derived assuming $y \sim o(R)$.

2.3. *Comparison with other approaches*

The non-parallel formulation (6) contains all terms nominally of $O(R^{-1})$ (except possibly for higher-order effects on the mean flow itself, which we shall consider below); by this we mean that no terms of higher order are retained, but, because of the occurrence of large gradients within the domain near the critical layer and the wall, further analysis may (and indeed will) reveal that all the terms retained may not necessarily make contributions of the same order to the solution. In other words, (6) provides a primitive equation entirely adequate for obtaining solutions to $O(R^{-1})$.

To compare (6) with other formulations, we consider the special case of flat-plate flow, for which $p = q$ and equation (6) reduces to

$$\{\mathrm{OS}\}\,\phi + \frac{q}{R}(a_3\mathrm{D}^3 + a_2\mathrm{D}^2 + a_1\mathrm{D} + a_0)\,\phi + a_\alpha\alpha'\phi + a_\phi\frac{\partial\phi}{\partial x} = 0, \tag{11}$$

where

$$a_3 = \Phi, \quad a_2 = \Phi', \quad a_1 = 2y\alpha(\omega - \alpha\Phi') - \alpha^2\Phi + \Phi'',$$

$$a_0 = -\alpha\omega + \Phi''', \quad a_\alpha = -\omega + 3\alpha\Phi', \quad a_\phi = \Phi''' + 3\alpha^2\Phi' - 2\alpha\omega - \Phi'\mathrm{D}^2.$$

It is shown in Appendix A that the equations of Barry & Ross, Ling & Reynolds and Sen are incomplete, i.e. they do not contain all the terms in (11), while the equation of Bertolotti *et al.* is consistent up to $O(R^{-1})$ with the above equation but contains in addition some terms of higher order (R^{-2}).

2.4. *Normalization*

The following factors must be clearly defined in a non-parallel stability analysis: the normalization adopted for ϕ; the flow quantity whose stability is being studied; the distance from the wall; and the path in the boundary layer along which the disturbance is being monitored. The disturbance streamfunction represented by equation (3) depends on x through both ϕ and α, hence there is an ambiguity in the apportioning of the x-dependence between them. By defining a normalization for ϕ, this ambiguity is eliminated. Although this normalization may be done in different ways and the wavenumber depends on the normalization chosen, determination of the stability (or otherwise) of a physical quantity will not be affected. Our choice here is the same as that used by Fasel & Konzelmann (1990) and by Bertolotti *et al.* (1992), and is defined by the condition that

$$\frac{\partial(\mathrm{D}\phi)}{\partial x} = 0 \quad \text{at the inner maximum of } \mathrm{D}\phi. \tag{12}$$

The inner and outer maxima are the first and second maxima encountered in the velocity eigenfunction when moving along the normal coordinate away from the wall. In spatial stability analysis using the parallel-flow assumption, disturbances of a given frequency are taken to be neutrally stable if the imaginary part of the wavenumber, α_i, is equal to zero. However in the non-parallel analysis the criterion can be written as

$$\frac{1}{Q}\frac{\partial Q(y_s)}{\partial x} = 0, \tag{13}$$

where Q is the physical quantity (usually either the disturbance kinetic energy or the streamwise or normal component of the disturbance velocity) whose value at the distance y_s above the wall is monitored along some prescribed path $y_s = y_s(x)$. For example, from the relation

$$\frac{1}{u_d'/U}\frac{\partial(u_d'/U)}{\partial x}\bigg|_y = \mathrm{Re}\left(\frac{\phi_{yx}}{\phi_y}\right)\bigg|_y - \alpha_i \tag{14}$$

(where the notation indicates evaluation at constant y) we see that the normalized velocity fluctuation of a given frequency may amplify at one y and decay at another. Also, corresponding expressions for different physical quantities show that at the same location one physical quantity may decay while another amplifies.

2.5. *Higher-order mean flow contribution*

In the above formulation, the mean flow was shown to satisfy the Falkner–Skan equation under the assumption that it obeys a similarity law in the non-dimensional coordinate y. However, this only gives the mean flow up to $O(1)$ while the disturbance terms are retained up to $O(R^{-1})$. A rational treatment of the stability problem therefore demands that the mean flow be also prescribed to $O(R^{-1})$. Now higher-order effects appear in the mean flow owing to various factors (see e.g. Van Dyke 1975), namely curvature, finite extent of the surface, vorticity in the outer flow, displacement thickness, etc. These effects are usually specific to the body in the flow, and hence do not lend themselves to a general analysis. Nevertheless, the present study may be considered to be on semi-infinite wedges in irrotational outer flow, or on a semi-infinite flat plate on which the free-stream velocity is arranged to follow a power law by the insertion of suitable surfaces elsewhere in the flow (such as liners on wind tunnel walls). In this case the only higher-order contribution to the mean flow is due to the displacement effect. To illustrate the influence of this effect on flow stability, the

contribution to the external velocity distribution on such a surface due to boundary-layer development (only) on that surface is obtained from thin-airfoil theory. A detailed analysis given in Appendix C yields

$$U(x) = U_0(x)\left(1+\frac{Hq}{R(x)\tan(\frac{1}{2}(m+1)\pi)}\right), \tag{15}$$

where the second term on the right is proportional to the displacement speed, H is the (constant) shape factor of the lowest-order velocity profile and $U_0 \propto x_d^m$. (It will be seen that the displacement speed is zero in Blasius flow, $m = 0$.) The higher-order velocity profile is shown in Appendix C to obey similarity in the Falkner–Skan variable. The mean velocity profile is given by

$$\frac{u_d}{U_0} = \Phi_0' + \frac{C}{R}\Phi_1', \tag{16}$$

where Φ_0 satisfies the Falkner–Skan equation (5),

$$C = Hq[\tan(\tfrac{1}{2}(m+1)\pi)]^{-1}$$

is a constant and $z = \Phi_1'$ obeys the equation

$$z'' + p\Phi_0 z' + (2q-p)[\Phi_0' z - 1] = 0. \tag{17}$$

The boundary conditions are

$$z = 0 \quad \text{at} \quad y = 0 \quad \text{and} \quad z = 1 \quad \text{as} \quad y \to \infty.$$

With the inclusion of the displacement effect the equation for the disturbance streamfunction (6) is modified to

$$\left[\{\mathrm{NP}\} + \frac{\mathrm{i}\alpha C}{R}(-\Phi_1' \mathrm{D}^2 + \Phi_1''' + \alpha^2\Phi_1')\right]\phi = 0, \tag{18}$$

which is now complete to $O(R^{-1})$ for the higher-order effect considered. Other higher-order contributions (such as curvature) would lead to additional terms in (18).

The boundary conditions remain the same as before.

3. Numerical method

Equation (6) can be treated like a parabolic equation and solved by a marching procedure, but we prefer a local approach that elucidates the connection with the Orr–Sommerfeld equation. For this purpose, a code for the computation of the eigenvalues of the Orr–Sommerfeld equation, developed by P. K. Sen (1989, personal communication), was modified to compute neutral stability curves for Falkner–Skan profiles based on (6). Details of the numerical method are given in Govindarajan (1994). The code uses the Thomas algorithm: equation (6) is discretized using central differencing, and a Noumerov transform is applied to give sixth-order accuracy on all the terms. This is done by writing the difference equation in terms of a new variable g given by

$$\phi_j = (1 + K_1\delta^2 + K_2\delta^4)g_j,$$

where δ stands (in this equation only) for the central-difference operator, and choosing K_1 and K_2 suitably. For a given α' and $\phi_x(y)$, a septa-diagonal matrix is obtained; the coefficients of the first three and last three rows are modified using the boundary conditions at the wall (7) and the far field (9) respectively. The matrix is solved by Gauss elimination with an assumed α and the correct eigenvalue is computed iteratively by the Newton–Raphson method. The procedure for computing $\partial\phi/\partial x$ and α' is as follows. First make some reasonable guess for $\partial\phi/\partial x$ and α' (e.g. from the

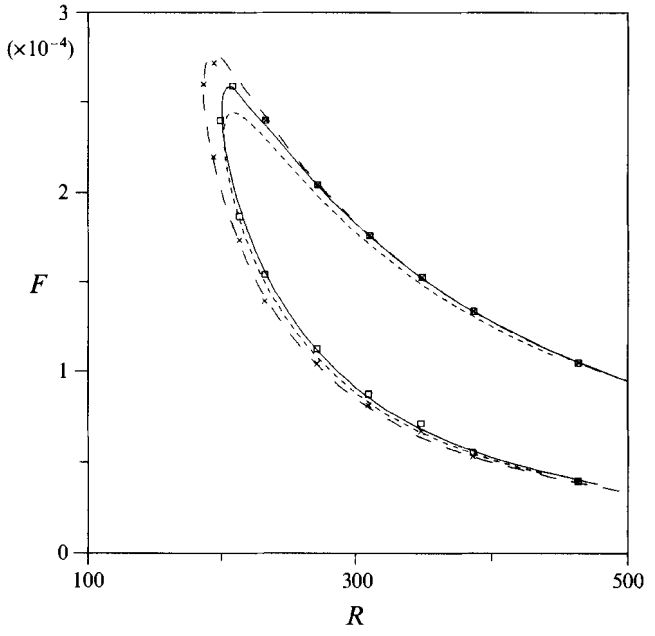

FIGURE 2. Comparison of present computations (—, inner maximum; – –, outer maximum) on a flat plate with Gaster (1974): □, inner maximum, ×, outer maximum; ----, Orr–Sommerfeld theory.

Orr–Sommerfeld solution), then solve (6) with the normalization (12) at x (or correspondingly, at R) for $\alpha(x)$ and $\phi(x)$ and at $x+\mathrm{d}x$ (or $R+\Delta R$) for $\alpha(x+\mathrm{d}x)$ and $\phi(x+\mathrm{d}x)$; compute $\partial\phi/\partial x$ and α' from the solution; repeat until these quantities converge. It is found that the solution converges within a few iterations.

The validation of the code is described in detail in Govindarajan (1994). The comparison with Gaster's results is shown in figure 2. The computational domain was about 2.4 times the boundary-layer thickness in the normal coordinate. The normalization condition (12) was satisfied by keeping $\mathrm{D}\phi$ at its inner maximum fixed at the complex constant $0.02+\mathrm{i}0$. The solution was assumed to have converged when the maximum difference (throughout the boundary layer) between the x-derivatives from successive iterations, say $(\Delta P)_{max}$, was less than 1×10^{-6}, where P stands for α', ϕ_x or $\mathrm{D}^2\phi_x$. The convergence was also assessed by computing the difference between the results when $(\Delta P)_{max}$ was 1×10^{-5} and 1×10^{-6}; the maximum difference occurred on the upper branch just below the maximum frequency, and was $\sim 0.15\%$. The value of ΔR within which the x-derivatives are assumed constant was taken as 0.1. On using a ΔR of 0.2 the results changed negligibly, the maximum deviation being $\sim 0.2\%$, again in the same region of the stability boundary.

The computational time in this 'local' method was about 1 s per step on a MIPS R3000 based machine. For comparison we also tried a marching procedure where the x-derivatives were computed from the known solutions at $R-\Delta R$ and R and used for the computation of the solution at $R+\Delta R$ (the solution at the initial location being computed using the local method). For the same computational step ΔR, the time taken by the local procedure is two to three times greater than that of marching. However, to get similar accuracy, the ΔR used for marching must be of the order of $1/20$ times the ΔR needed for the local procedure, so for the same accuracy the local procedure is five to six times faster than the marching procedure. The local procedure

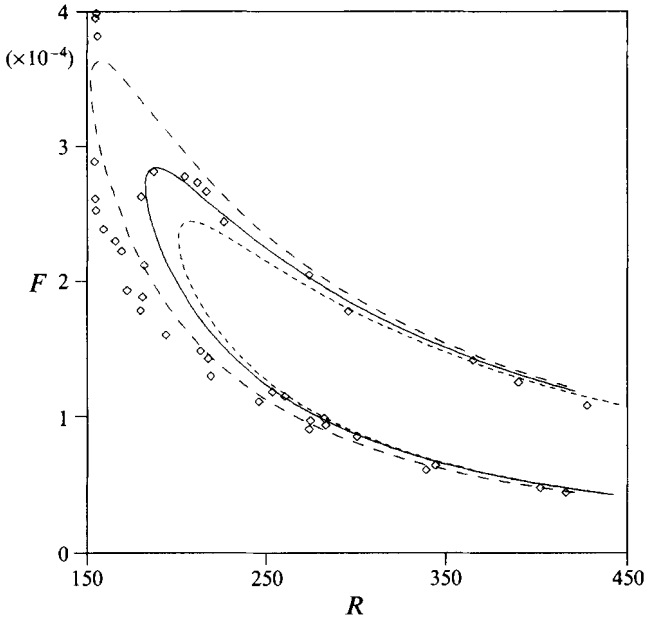

FIGURE 3. Neutral stability curves at constant y: ——, $y_a/\delta = 0.05$; —, $y_a/\delta = 0.15$; ----, Orr–Sommerfeld; ◇, Ross *et al.* (1970).

is even more economical in the computation of neutral stability boundaries because there is no need to follow a particular frequency until neutral stability. Bertolotti *et al.* use a spectral method and their 'marching' and 'local' procedures are different from the ones used here; e.g. in their marching procedure, Bertolotti *et al.* iterate for the correct value of the streamwise variation of the wavenumber by imposing the normalization condition and are able to use a larger ΔR than in the marching procedure here. Since a direct comparison of computational times per step is not meaningful, we compare the times taken for a given accuracy. This is done by following the frequency $F = 8.6 \times 10^{-5}$ (which is the case studied by Bertolotti 1991) from a Reynolds number below the lower boundary ($R = 308$) to one above the upper boundary ($R = 565$). The standard solution is taken to be the one using $\Delta R = 1$ (256 steps). The deviation in the solution at the final Reynolds number from the standard solution is of the order of 10^{-6} up to $\Delta R = 8$, and $\sim 10^{-5}$ for $\Delta R = 16$, beyond which the solution rapidly deteriorates. The accuracy and computational time (taking machine speeds into account) for following a given frequency are about the same as those obtained by Bertolotti *et al.* However, the local method used here is faster for the computation of stability boundaries.

The assumption that α' and $\partial\phi/\partial x$ are $O(R^{-1})$ and α'' and $\partial^2\phi/\partial x^2$ are $o(R^{-1})$ was assessed numerically for $m = -0.06$ by following a disturbance of frequency $F = 2.265 \times 10^{-4}$ from $R = 70$ to 140. The maximum value of $R|\alpha'/\alpha|$ encountered was 0.31 and the quantity

$$\max_y \left| \frac{R}{\phi} \frac{\partial \phi}{\partial x} \right|$$

was less than 1.1 for all R. The largest values of $R|\alpha''/\alpha|$ and

$$\left| \frac{R}{\phi} \frac{\partial^2 \phi}{\partial x^2} \right|$$

were 10^{-4} and 0.03 respectively.

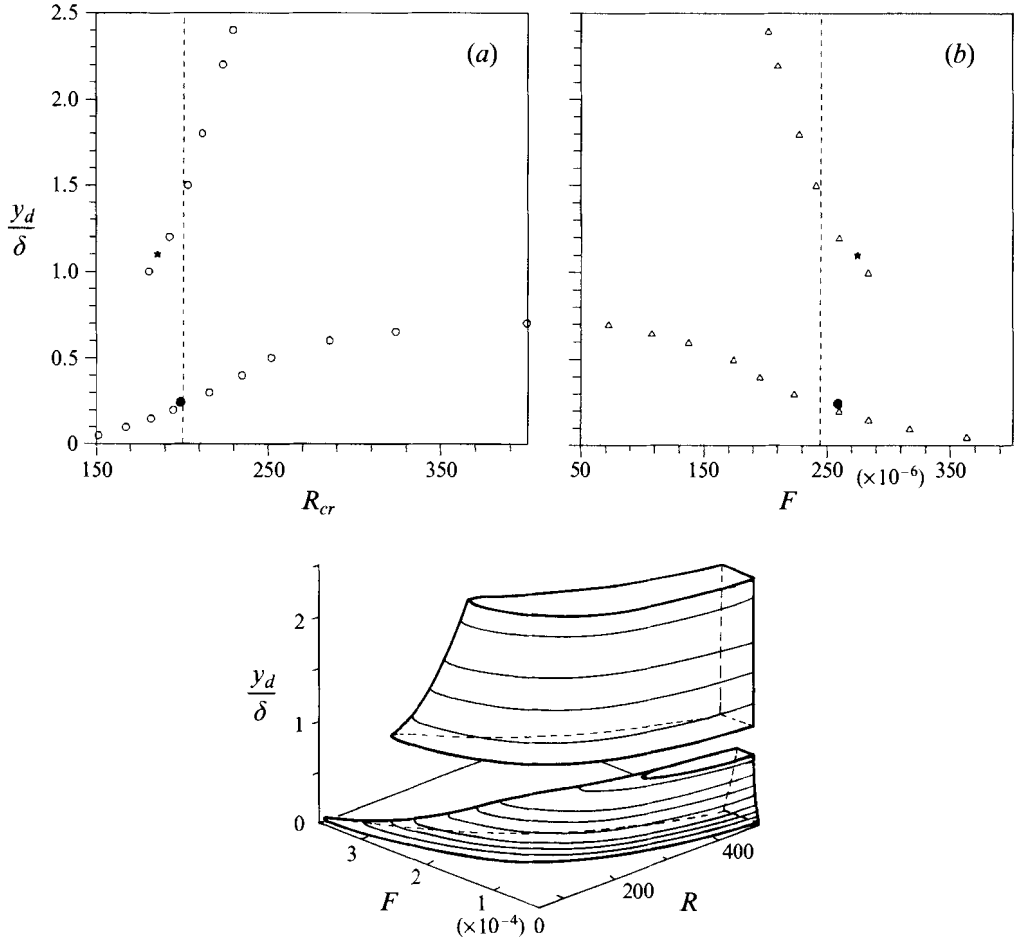

FIGURE 4. Dependence of (*a*) critical Reynolds number (○) and (*b*) maximum unstable frequency (△) on distance from wall from the Blasius boundary layer: ●, inner maximum; *, outer maximum; ----, Orr–Sommerfeld. (*c*) View of stability surface of Blasius boundary layer in (y, F, R)-space.

4. Effect of non-parallel formulation on neutral stability

The experiments of Ross *et al.* (1970) mapped the neutral boundary for the streamwise velocity fluctuations monitored at about $y_d = 0.15\delta$ where δ is the boundary-layer thickness; we take it here as the height where $u_d/U = 0.99$. The corresponding theoretical predictions from the present work are shown in figure 3. It is seen that the discrepancy between experiment and linear stability theory is not reduced substantially by the inclusion of non-parallel effects. However (as has been pointed out by several workers, e.g. Fasel & Konzelmann 1990), stability is very sensitive to the distance of the monitoring location from the surface, which calls for experiments where the measured quantity and the path followed by the measuring probe are specified accurately. This point is illustrated by the close agreement between the stability boundary for $y_d/\delta = 0.05$ and experiment (figure 3). The extreme sensitivity to the normal distance is obvious from figure 4, which shows the critical Reynolds number and the maximum unstable frequency obtained from the stability diagrams of u' along constant-y paths as functions of y_d/δ. In non-parallel flow theory the stability boundary (for any given flow quantity) is a two-dimensional surface in the

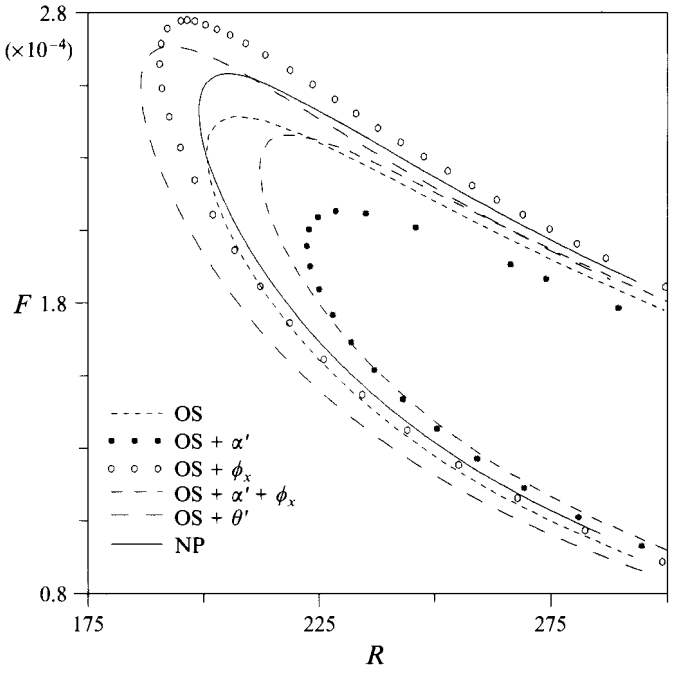

FIGURE 5. Contribution of various terms to the stability boundary at the inner maximum in Blasius flow.

three-dimensional (y, F, R)-space; a representation of this surface is shown in figure 4(*c*). A sharp discontinuity is obtained near the location of phase change in the streamwise disturbance velocity, which is consistent with the observations of Fasel & Konzelmann, who plot the neutral Reynolds number for a disturbance of frequency $F = 3 \times 10^{-4}$ as a function of the distance from the wall.

The stability of the streamwise velocity at its (inner) maximum has received a lot of attention in most non-parallel studies. This is because the height at which the amplitudes are largest is believed to be the most likely location for the onset of nonlinear interactions and breakdown to turbulence. The neutral stability curve for the streamwise velocity perturbations at the inner maximum is seen (figure 2) to deviate very little from the parallel-flow result. In view of the sensitive dependence on y of the stability boundary, it must be considered a coincidence that the values at the inner maximum lie so close to the predictions made by the parallel analysis.

To understand the cause of the differences seen in figure 2, we first note that equation (11) can be written as

$$\{\mathrm{OS}\}[\phi] + \theta' a_\theta[\phi] + \alpha' a_\alpha[\phi] + a_\phi[\partial\phi/\partial x] = 0, \tag{19}$$

where

$$a_\theta = a_3 \mathrm{D}^3 + a_2 \mathrm{D}^2 + a_1 \mathrm{D} + a_0.$$

It can be seen from (19) that the non-parallel effects can be conveniently attributed to three types of terms, respectively proportional to the streamwise variation of the boundary-layer thickness (θ'), the wavenumber (α') and the eigenfunction ($\partial\phi/\partial x$). The question that arises is whether the contribution of each of these terms is negligible, or whether the terms tend to counteract each other. To answer this question the effect of each of these terms relative to the Orr–Sommerfeld solution was studied separately. Figure 5 shows that the $\partial\phi/\partial x$ term has a destabilizing effect while the α' term is

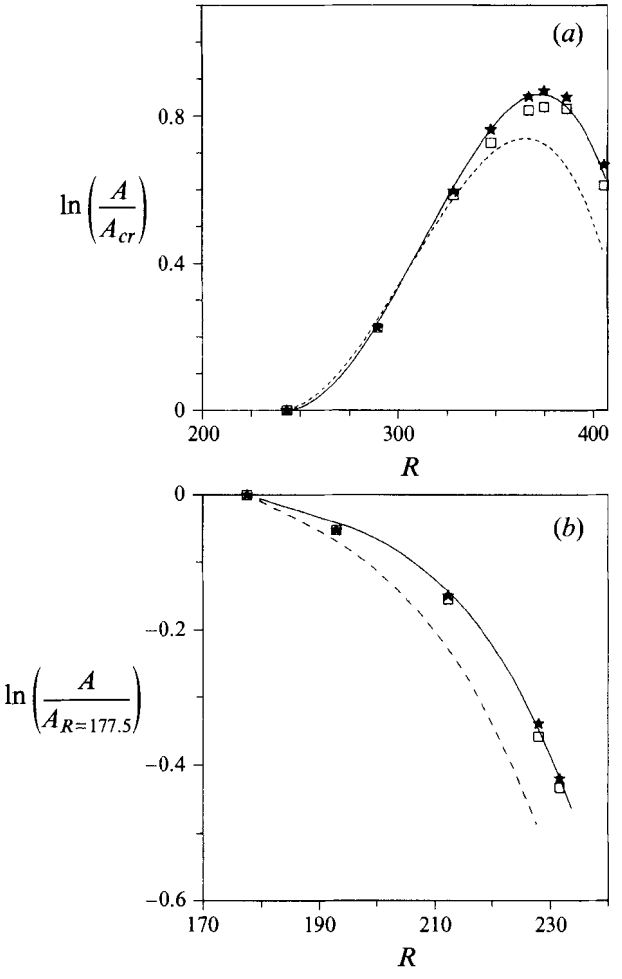

FIGURE 6. Amplitude ratios at the inner maximum in Blasius flow: ——, present; ----, Orr–Sommerfeld; □, Gaster (1974); ★, Fasel & Konzelmann (1990). (*a*) $F = 1.4 \times 10^{-4}$, (*b*) $F = 3 \times 10^{-4}$.

stabilizing. Since the distribution of the x-dependence between the eigenfunction (ϕ) and the exponent (α) is arbitrary, it is only the joint contribution of the two that is physically relevant. This joint effect is seen from figure 5 to be slightly stabilizing, while there is an increase in the unstable region when the θ' term alone is added to the Orr–Sommerfeld equation. Thus, although each non-parallel term has a significant effect on the stability, their effects at the inner maximum tend to counteract each other to give a final stability boundary very close to the Orr–Sommerfeld loop.

Figure 6 shows that amplitude ratios computed by the present theory are in good agreement with the direct simulations of Fasel & Konzelmann. At the inner maximum (figure 6*a*), the present results agree even more closely with the direct numerical simulations than those of Gaster at $F = 1.4 \times 10^{-4}$ (figure 6*a*), while all three results agree very well at $F = 3 \times 10^{-4}$ (figure 6*b*).

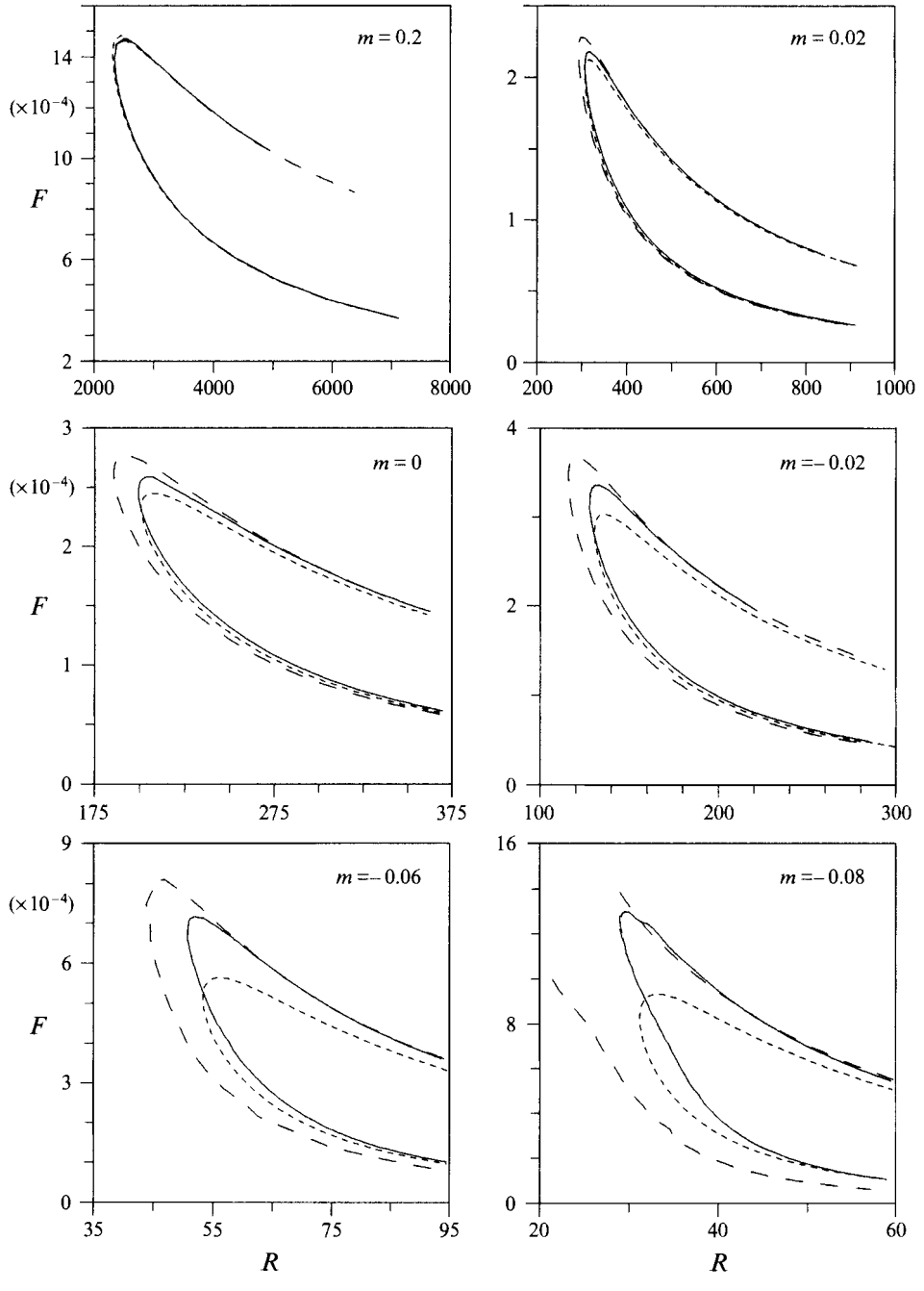

FIGURE 7. Non-parallel effects on the stability boundary in Falkner–Skan flows. ----, Parallel flow. Present results: —, inner maximum; – –, outer maximum.

5. Results for Falkner–Skan flows

Stability boundaries have been computed for different values of the Falkner–Skan parameter m, and a representative sample is shown in figure 7. The non-dimensional frequency plotted in these figures is given by $F = \omega/R^{(1-3m)/(1+m)}$, which is proportional to the dimensional frequency ω_d. At high negative values of m, i.e. close to separation,

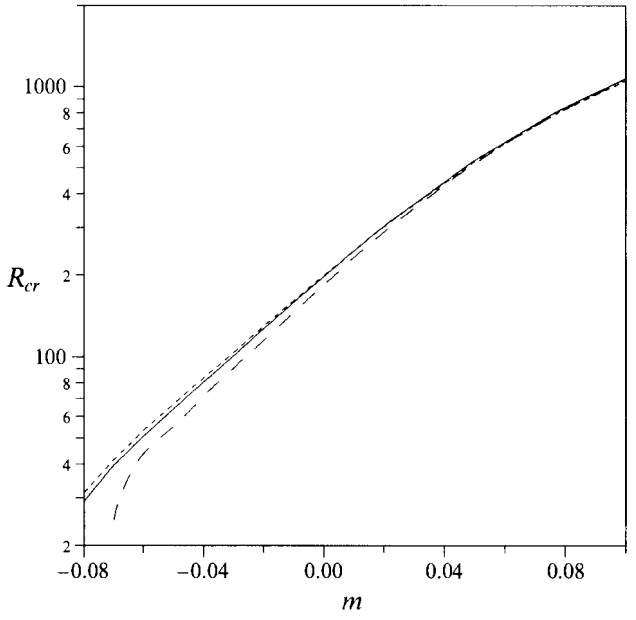

FIGURE 8. Effect of flow non-parallelism on the critical Reynolds number of Falkner–Skan flows. ----, Parallel flow. Present results: —, inner maximum; – –, outer maximum.

numerical convergence became more and more difficult, and the criterion for convergence had to be relaxed by an order of magnitude for $m = -0.08$. However, since the critical Reynolds number is an order of magnitude smaller at this value of m than in zero-pressure-gradient flows, the relative magnitude of the error (ΔP) and the reciprocal of the Reynolds number remain the same. In favourable pressure gradients, the present results are hardly different from the parallel-flow theory, as seen from figure 7. This is understandable as the Reynolds numbers encountered are so high that $1/R$ effects are bound to be smaller. Shown in the same figure are the non-parallel effects in adverse-pressure-gradient flows. Here, the reduction in critical Reynolds number is significant. At $m = -0.08$ there were convergence difficulties at low Reynolds numbers as already mentioned, so no closed loop is shown. The effect of the new non-parallel terms in the stability equation on the critical Reynolds number increases with increasing adverse pressure gradient, as shown in figure 8.

The higher-order mean flow equation (17) may be solved for different values of m, and an example of the results is shown in Appendix C. For $m \leqslant 0.082$ the higher-order profile contains a region of negative contribution to the velocity, but the total streamwise velocity does not contain any reverse flow for $m \geqslant -0.08$. In the case of flow over a flat plate, $C = 0$ and there is no first-order correction to the mean flow due to displacement thickness, although equation (17) can be solved for $m = 0$ to give a z-distribution. The effect of the higher-order mean flow is negligible in favourable-pressure-gradient flows, once again because of the high Reynolds numbers involved. In adverse pressure gradients the coefficient C is a (numerically small) positive quantity, and the higher-order velocity profile has a destabilizing effect since it reduces the velocity near the wall. It is seen from figure 9 that the effect is significant in strong pressure gradients at low Reynolds numbers.

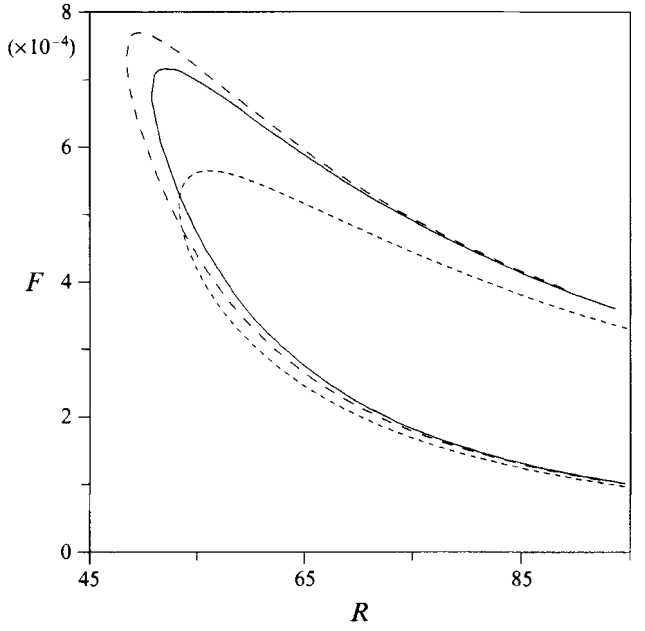

FIGURE 9. Change in stability boundary at the inner maximum due to higher-order displacement effect on the mean flow at $m = -0.06$. ----, Orr–Sommerfeld; —, non-parallel, Falkner–Skan solution; – –, non-parallel, including displacement effect.

6. Implications for e^n methodology

The maximum amplitude ratio n is defined by

$$n = \max_F \{\log(A/A_{cr})\}, \tag{20}$$

where A is the amplitude at a given location of a disturbance of a certain frequency and A_{cr} is the amplitude at the critical Reynolds number, and the maximum is taken over all frequencies. Since the work of Smith & Gamberoni (1956) and Van Ingen (1956), the factor n has been widely used in semi-empirical methods for the prediction of transition onset in boundary layers. Recent flight work (Horstmann, Quast & Redekar 1990) suggests that although n is not a constant at transition, there does appear to exist a good correlation between the value of n and transition Reynolds number.

In the present formulation, A for streamwise velocity fluctuations is given by

$$\frac{u'/U}{(u'/U)_{cr}} = \frac{A}{A_{cr}} = \mathrm{Re}\left\{\frac{\mathrm{D}\phi}{[\mathrm{D}\phi]_{cr}} \exp\left(\mathrm{i}\int_{x_{cr}}^{x} \alpha \,\mathrm{d}x\right)\right\}.$$

Hence, at the inner maximum where $\mathrm{D}\phi$ is held constant due to the normalization used, (20) reduces to

$$n = \max\left[\frac{-1}{p}\int_{R_{cr}}^{R} \alpha_i \,\mathrm{d}R\right].$$

Figures 10 and 11 show the amplitude ratios at the inner and outer maxima for various values of the Falkner–Skan parameter m. It is seen that individual amplification curves at higher frequencies depart significantly from the parallel-flow computations. For example, from figure 10 for $m = 0$ it is seen that for $F = 1.33 \times 10^{-4}$, the logarithm of the maximum amplification from a non-parallel analysis is higher than the parallel result by about 15% and 30% at the inner and outer maxima respectively. For $m =$

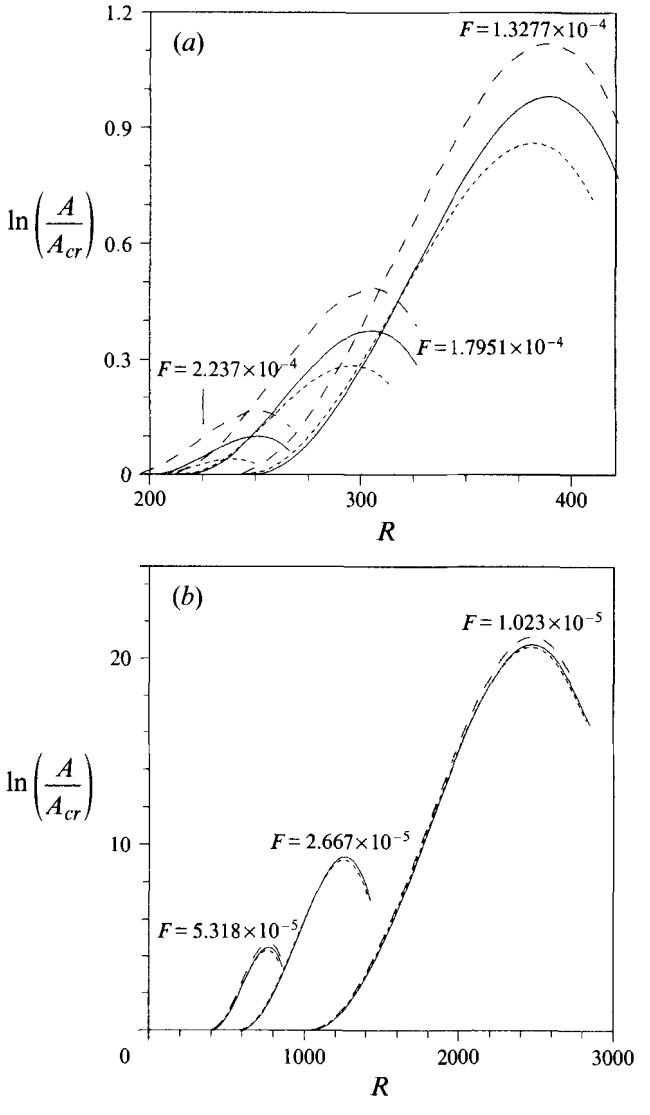

FIGURE 10. Amplification factors at different frequencies and $m = 0$. (*a*) Low Reynolds numbers; (*b*) high Reynolds numbers. ----, Orr–Sommerfeld; —, inner maximum; – –, outer maximum.

-0.06 (figure 11), $F = 2.52 \times 10^{-4}$ gives rise to amplification ratios whose logarithms are 20% and 40% greater than the parallel result at the inner and outer maxima respectively. For disturbances of low frequencies (high Reynolds numbers), however, there is no significant difference between parallel and non-parallel results.

The envelope of the amplification curves (n) is shown in figure 12. It is seen that although the amplification of individual frequencies especially at low Reynolds numbers is substantially altered by non-parallel effects, n at the inner maximum is not changed significantly: the maximum difference in n due to flow non-parallelism is 0.05, which is well within the uncertainties of the whole e^n methodology. For transition predictions by the e^n method, where the speed of the computational method is an important factor, n_P obtained from the parallel analysis should therefore be sufficient for most practical purposes. The fact that amplitude ratios are affected by non-

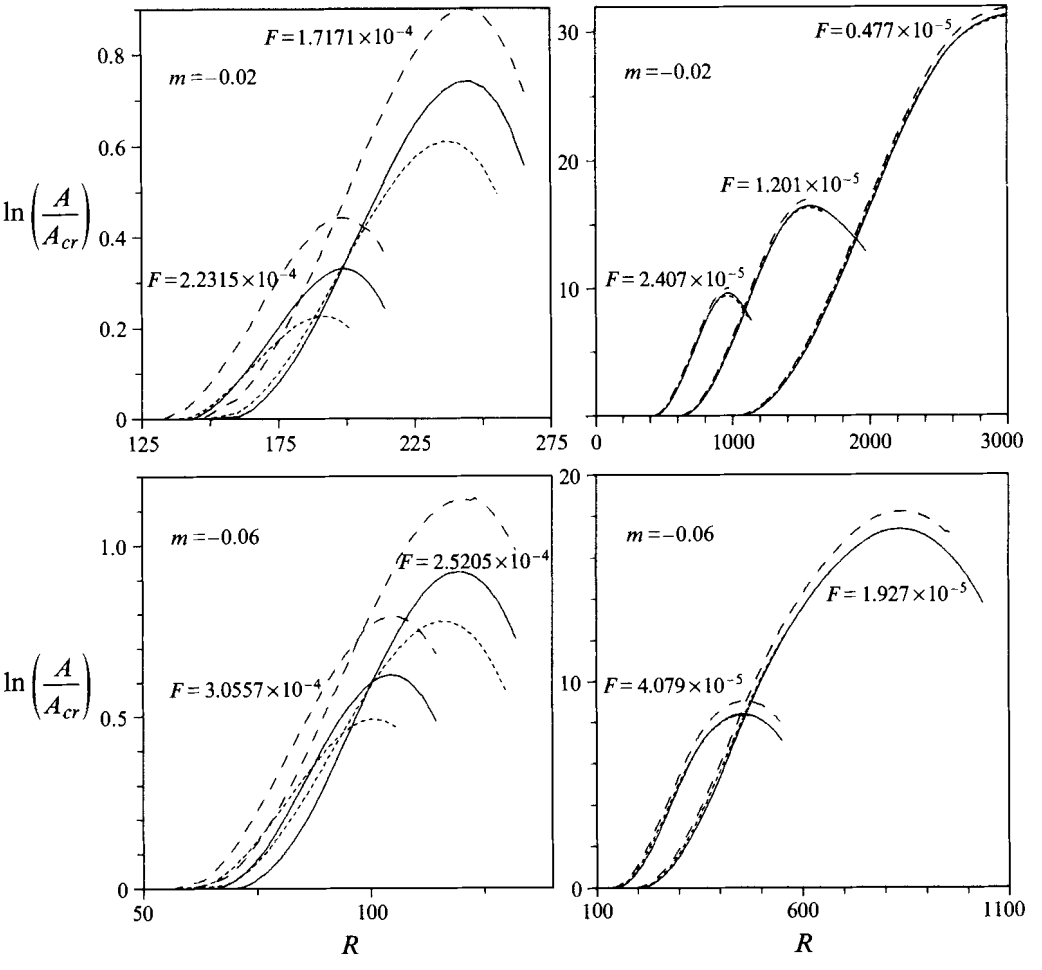

FIGURE 11. Amplification factors in adverse pressure gradient flows (legend same as in figure 10).

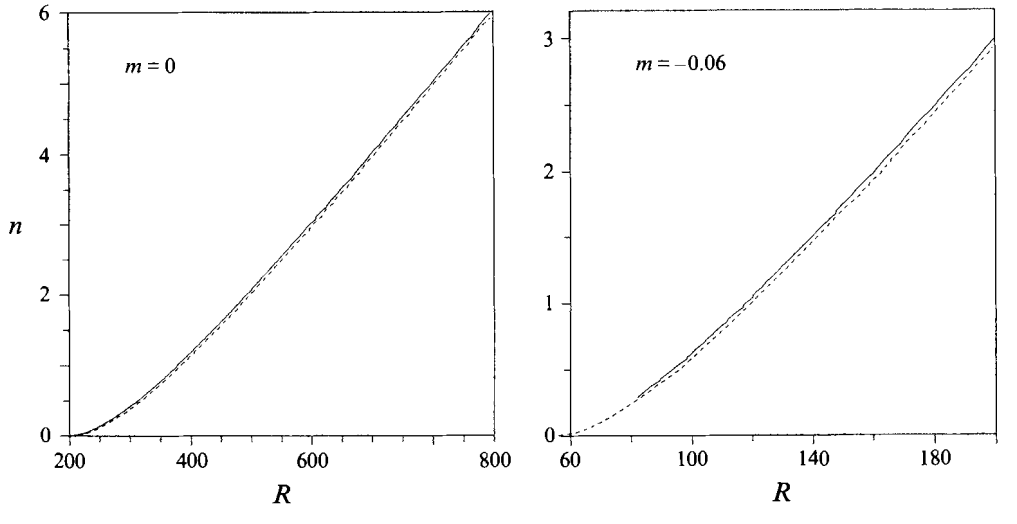

FIGURE 12. Amplification envelopes: ----, Orr–Sommerfeld; —, inner maximum.

parallelism only when they are relatively low implies that corrections may be necessary only in highly disturbed environments where transition Reynolds numbers are low, e.g. in turbomachinery applications. Special note of non-parallel effects should be taken in situations where the noise contains a dominant frequency at the high end of the unstable range.

7. Formulation for arbitrary pressure gradients

If the boundary layer does not follow one of the similarity solutions there are several approaches one can take. The most obvious one is to solve for the mean flow by one of the many algorithms now available (e.g. Cebeci & Smith 1974), and analyse its stability through the analogue of equation (6), generalized for arbitrary pressure gradient. However, in many applications it is usually possible to use a local similarity or near-similarity approach, as this lends itself to faster calculation procedures and provides greater insight into the stability results. We follow here the latter approach, and illustrate its use in a specific case.

In the present approach, it is useful to begin by introducing the pressure gradient parameter λ defined by Thwaites (1949), and write the gradient of the free-stream velocity U as

$$\frac{\mathrm{d}U}{\mathrm{d}x_a} = \frac{\lambda U}{R\theta}. \tag{21}$$

It turns out to be sufficient to compute the momentum thickness by a modification of the Thwaites relation due to Dey & Narasimha (1990),

$$\theta^2 = \frac{0.44\nu}{U^{5.4}} \int_0^{x_a} U^{4.4}\,\mathrm{d}x_a, \tag{22}$$

in which the exponents have been chosen to give good agreement over a wider range of pressure gradients than those originally considered by Thwaites (especially highly favourable gradients). On comparing (21) and (22) with (4) it is seen that

$$p = 0.22 - 1.7\lambda \quad \text{and} \quad q = 0.22 - 2.7\lambda. \tag{23}$$

As λ is in general a function of x_a, p and q are no longer constant as for similar flows, but for flows where λ varies slowly in x, i.e.

$$\frac{\mathrm{d}\lambda}{\mathrm{d}x_a} \sim O(R^{-1}),$$

their derivatives with respect to x may be neglected. This consideration allows us to compute the mean flow in the non-similar boundary layer in a simple way, through the mean streamfunction Φ introduced in (3), except that it is now a function of both x and y with an x-derivative of $O(R^{-1})$. On making use of this approximation in equation (2), the mean flow equation becomes

$$\mathrm{D}^4\Phi + p\Phi\mathrm{D}^3\Phi + (2q-p)\,\mathrm{D}\Phi\mathrm{D}^2\Phi = R[\mathrm{D}\Phi\mathrm{D}^2 - \mathrm{D}^3\Phi]\,\partial\Phi/\partial x,$$

which can be integrated once with respect to y to give

$$\mathrm{D}^3\Phi + p\Phi\mathrm{D}^2\Phi + (p-q)[1-(\mathrm{D}\Phi)^2] = R(\mathrm{D}\Phi\mathrm{D} - \mathrm{D}^2\Phi)\,\partial\Phi/\partial x. \tag{24}$$

The corresponding disturbance equation is

$$\{\mathrm{NP}\} + \left[\frac{\partial\Phi}{\partial x}\mathrm{D}^3 - (\alpha^2 + \mathrm{D}^2)\frac{\partial\Phi}{\partial x}\mathrm{D}\right]\phi = 0. \tag{25}$$

Equations (24) and (25) are now solved using the algorithms described in §3.

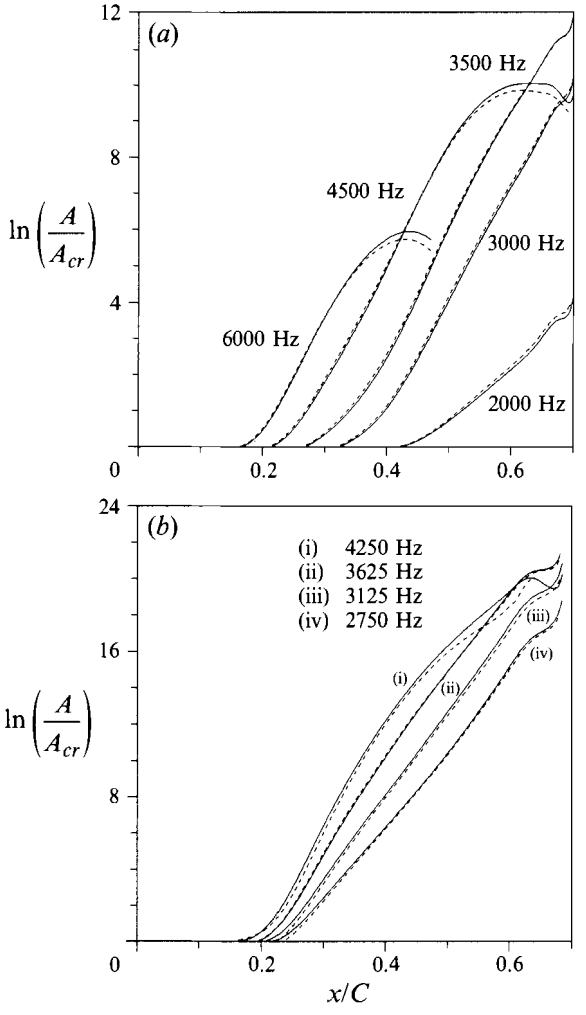

FIGURE 13. Amplification factors on a DESB159 airfoil at a Reynolds number of 10^6. (*a*) Angle of attack = −0.954°, (*b*) 1.279°. ----, Orr–Sommerfeld; —, inner maximum.

In order to assess the implications of the non-parallel formulation for pressure gradient flows of the kind often encountered in applications, especially in airfoil analysis and design, we have solved equations (24) and (25) for the airfoil DESB159, which has been analysed extensively by Viken (1986). This section is typical of a class of natural laminar-flow airfoils designed with the help of linear stability theory, and has been tailored to give a desired amplification at the design condition using only as much acceleration as is necessary, so that the severity of the downstream pressure recovery is reduced to the minimum. At the design condition of $C_L = 0.45$ (angle of attack = −0.954°), the amplitude ratios computed from parallel theory at a chord Reynolds number of 1×10^6 agree closely with Viken's results (the largest difference being 0.6 at a frequency of 6000 Hz), although the pressure distribution on the airfoil was taken from a diagram and so was not accurately known. The mean flow was calculated from equation (24). On performing a non-parallel stability analysis on this airfoil, the difference in the amplitude ratios was not significant (figure 13*a*). This

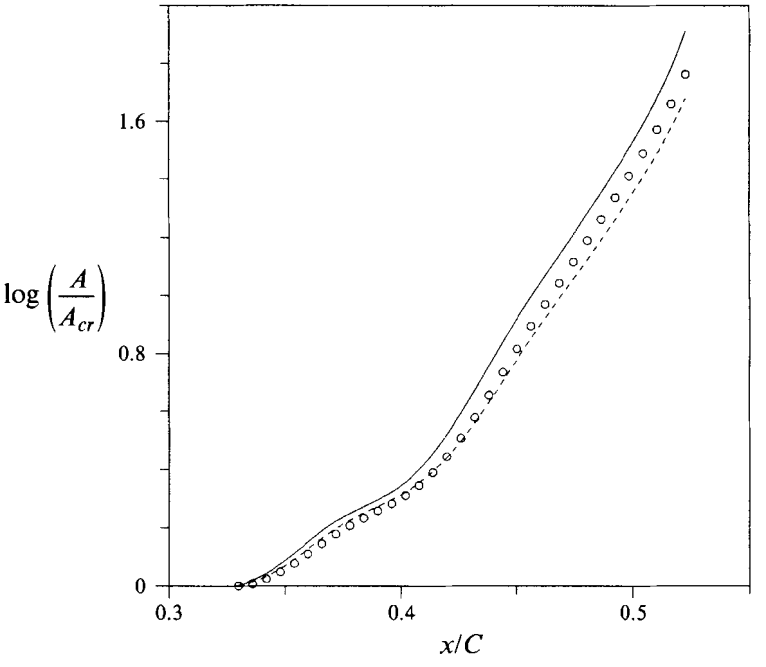

FIGURE 14. Amplification factors on a Wortmann FX-63-137 airfoil. Angle of attack = 0, chord Reynolds number = 80000. ----, Orr–Sommerfeld; ○, non-parallel (local similarity); —, non-parallel (weakly non-similar).

observation is also true for the off-design condition of $C_L = 0.75$, as may be seen from figure 13(*b*).

On the other hand, we obtain slightly different results for the Wortmann FX-63-137 airfoil (Miley 1982), also designed for natural laminar flow applications, when we analyse the flow at low Reynolds numbers. The mean flow here was computed as before, by solving (24). The results from two different approximate analyses are shown in figure 14. In the first, which we shall call the local similarity approximation, the amplitude ratios are computed from equation (6), with the local value of the parameters p and q obtained from (23). In the second, which we shall call the weakly non-similar approach, the mean flow is computed from (24) and the stability characteristics from (25). It is seen that the non-parallel effects are significant at low Reynolds numbers; the amplitude ratios computed from the weakly non-similar theory are consistently higher than those from either the parallel theory (by up to 0.2) or the local similarity approach at a chord Reynolds number of 80000. At a Reynolds number of 2×10^6, however, the differences cannot be considered significant for applications. Airfoils which are designed to operate at low Reynolds numbers, especially those in high-disturbance environments where transition also takes place at low Reynolds numbers, would require a non-parallel analysis such as that proposed by equation (25) for accurate computations of amplitude ratios. However, this analysis does not account for surface curvature, which could alter the results significantly.

8. Lowest-order non-parallel flow theory

Considering that the effects of non-parallelism as discussed above, especially for calculations of total amplification, are in general weak, and no more than modest even in strong adverse pressure gradients, it is pertinent to ask what a rational $O(1)$ estimate

of the stability characteristics of a (spatially growing) boundary layer would be. A related consideration is the following. If we propose to estimate stability parameters to $O(R^{-1})$, it is clearly necessary to first have the mean flow correct to $O(R^{-1})$, i.e. to work with higher-order boundary-layer theory (as we have already illustrated in §2.5). However, it surely is not acceptable to argue that non-parallel effects can be rationally estimated only when higher-order boundary-layer velocity profiles are available. It is true that this question does not arise in the special case of Blasius flow on an infinite flat plate, as the higher-order solution in this case happens to vanish; but in general this is not true, and we should expect to be able to formulate a lower-order non-parallel flow theory.

To pursue this question, we begin by noting that all variables in (6), including x, y and α, already contain some information about the non-parallel flow in the boundary layer. In the limit of large R we may at first expect only the inviscid terms in (6) (constituting the Rayleigh equation in transformed variables),

$$\{\mathrm{i}(\omega-\alpha\Phi')\,\mathrm{D}^2+\mathrm{i}\alpha[-\alpha(\omega-\alpha\Phi')+\Phi''']\}\,\phi=0,$$

to govern the eigenfunction ϕ, but it is well known from Tollmien–Schlichting theory that, because of the singularity at the critical layer and the no-slip condition at the wall, viscous layers appear in the solution, to which they make $O(1)$ contributions. The terms that describe these viscous layers are already known from Orr–Sommerfeld theory; all the other terms in (6) (in particular those proportional to θ', α' and ϕ_x) make only higher-order contributions to the solution. However, not all the terms in the Orr–Sommerfeld equation are equally significant either, as the following argument shows. At large R, classical arguments can be repeated to show that (in the transformed variables also) the critical layer and the wall layer have thicknesses that are respectively proportional to $R^{-1/3}$ and $R^{-1/2}$; under certain conditions the former may be contained in the latter (see e.g. Drazin & Reid 1981; Graebel 1966). Now writing the Orr–Sommerfeld equation in the form

$$[-\mathrm{i}(\omega-\alpha\Phi')\,\mathrm{D}^2+\mathrm{i}\alpha\{\alpha(\omega-\alpha\Phi')-\Phi'''\}]\,\phi=\frac{1}{R}[\mathrm{D}^4-2\alpha^2\mathrm{D}^2+\alpha^4]\,\phi$$

we see from an order-of-magnitude analysis that, in the critical layer, the terms are respectively of order 1 and $R^{-1/3}$ on the left, and 1, $R^{-2/3}$ and $R^{-4/3}$ on the right. Now as we are limiting ourselves to the lowest-order basic flow which is known only to less than $O(R^{-1})$, terms of this and higher order cannot legitimately be retained in a rational analysis to the lowest order. We therefore have the valid limiting equation

$$-\mathrm{i}(\omega-\alpha\Phi')\,\mathrm{D}^2\phi=\frac{1}{R}\mathrm{D}^4\phi+\left[\mathrm{i}\alpha(-\alpha(\omega-\alpha\Phi')+\Phi''')-\frac{2\alpha^2}{R}\mathrm{D}^2\right]\phi,$$

where the square brackets contain terms which can be neglected to $O(1)$, but may be retained to $O(R^{-2/3})$. It is well known that their retention is necessary for matching the critical layer to inviscid-layer solutions (Drazin & Reid 1981).

A similar analysis shows that the only terms of order lower than R^{-1} in the wall layer are

$$-\mathrm{i}(\omega-\alpha\Phi')\,\mathrm{D}^2\phi=\frac{1}{R}\mathrm{D}^4\phi.$$

Clearly therefore the term $\alpha^4\phi/R$ in the Orr–Sommerfeld equation ought to be

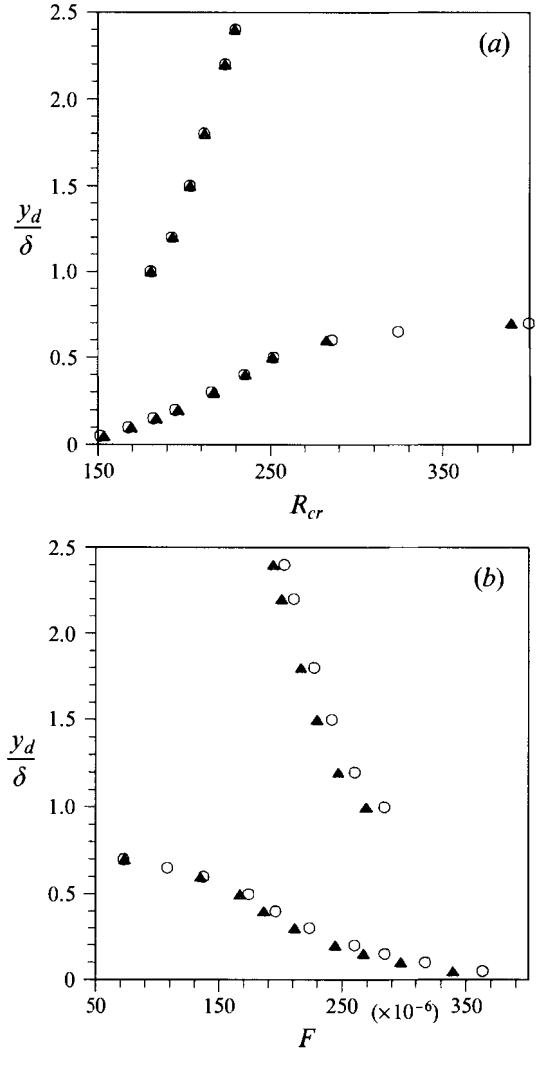

FIGURE 15. Dependence of (*a*) critical Reynolds number and (*b*) maximum unstable frequency on distance from wall. ○, Full non-parallel theory to $O(R^{-1})$; ▲, lowest order non-parallel theory (reduced Orr–Sommerfeld).

removed, as it is of higher order everywhere. All the relevant 'distinguished' limits of the problem can therefore be obtained from the 'reduced' Orr–Sommerfeld equation

$$\{\mathrm{OS}\}'\phi \equiv \left[\mathrm{i}(\omega-\alpha\Phi')(\mathrm{D}^2-\alpha^2)+\mathrm{i}\alpha\Phi'''+\frac{1}{R}(\mathrm{D}^4-2\alpha^2\mathrm{D}^2)\right]\phi = 0. \tag{26}$$

This is therefore a rational approximation to similar flows with the streamfunction decomposition (3), valid also for non-similar flows as defined in §7 (equation (25) contains no additional low-order terms). Thus, equation (26) governs the stability of *non-parallel* boundary-layer flows in the lowest order, provided the variables (which resemble those that appear in the classical Orr–Sommerfeld equation) are interpreted in the light of the transformations (3). In the literature to date, the Orr–Sommerfeld equation and the parallel-flow assumption have been treated as synonymous. What we

have demonstrated is that, in *transformed* variables, the (reduced) Orr–Sommerfeld equation already provides the lowest-order solution in non-parallel flow.

To verify this assertion, we have computed solutions of (26) and obtained stability boundaries using (14). Note that in (26) R is a function of x, the eigensolution $\phi = \phi(y; R(x))$ contains $R(x)$ implicitly as a parameter, and

$$\frac{\partial \phi}{\partial x} = \frac{\partial \phi}{\partial R}\bigg|_y \frac{\mathrm{d}R}{\mathrm{d}x};$$

substituting this relation in (14) the variation of the stability characteristics in y (characteristic of the non-parallel flow) can be worked out. The results are shown in figure 15, in comparison with the higher-order calculations of §4, for the special case of Blasius flow: it is seen that the agreement is satisfactory. The fact that a reinterpreted Orr–Sommerfeld equation (reduced or otherwise) implicitly contains information on the effects of non-parallelism is presumably the reason for the success of Gaster's method for handling the problem.

It has been numerically confirmed that a solution of equation (26) shows virtually no difference from that of the Orr–Sommerfeld equation for all the Falkner–Skan flows considered here.

An important consequence of the absence of $\alpha^4\phi/R$ in (26) is that the reduced form of the partial differential equations that imply the (reduced) Orr–Sommerfeld equation are no longer elliptic. A full exploration of the consequences of the ideas set forth in this section will be separately published.

9. Conclusions

A rational formulation for the stability of similar boundary layers, taking account of non-parallelism in the flow and correct to $O(R^{-1})$, has been proposed. The present non-parallel analysis confirms that stability is a sensitive function of the normal distance from the surface. If we choose amplification at the inner maximum of the streamwise velocity perturbation as the criterion for stability, the present results are very close to those of parallel theory for Blasius flow, but this must be considered somewhat of a coincidence as the agreement would disappear if a different location or criterion were specified. Adopting the inner maximum criterion, the differences between parallel and non-parallel theory are even less when the pressure gradient is favourable, but there is a significant departure at low Reynolds numbers in decelerating flows. The higher-order mean velocity profile due to the displacement effect has a negligible effect in favourable-pressure-gradient flows, but an appreciable destabilizing effect at low Reynolds numbers in strong adverse pressure gradients. The amplification curves for individual frequencies in zero and adverse pressure gradients change substantially at low Reynolds numbers at both the inner and outer maxima. Their envelope at the inner maximum, however, changes only marginally, the n factor being different by at most 0.05 in adverse-pressure-gradient flows.

We wish to point out that owing to the use of the transformed coordinates (3) in the present approach, it is straightforward to eliminate higher-order terms and arrive at a rational formulation up to any desired order. Furthermore, our representation does not make use of a reference point (such as R_0 in equation (6) of Bertolotti *et al.*) and is therefore a more efficient way of computing local solutions. We have demonstrated that the present equation may also be treated as a parabolic equation and solved by space marching, if necessary, although this has no advantage in mapping stability boundaries. Nonlinear effects can also be handled, as we propose to show subsequently.

It is important to distinguish the present approach from other high-Reynolds-number asymptotic theories such as the triple-deck theory of Smith (1979), which is not valid at moderately high Reynolds numbers. Thus, while the triple-deck results compare well with the present results for flat-plate flow at very high Reynolds numbers, there are significant differences at the lower Reynolds number end of the stability boundary (the triple-deck theory does not yield a critical Reynolds number). Indeed, as critical Reynolds numbers even in the presence of significantly adverse pressure gradients are $\gg 1$, the entire stability loop can be predicted accurately by the present method for all pressure gradients.

Finally, we have shown that the lowest-order effects of non-parallelism are in fact already present in a suitably reinterpreted version of a reduced Orr–Sommerfeld equation; for similarity solutions of the boundary-layer equations, the reinterpretation consists in the use of local non-dimensionalization exactly as in the Falkner–Skan equations. In such appropriately transformed variables, the (reduced) Orr–Sommerfeld equation already provides the lowest-order rational estimates of the stability parameters of a growing boundary layer; these should be satisfactory in applications except possibly when transition occurs at relatively low Reynolds numbers in the presence of adverse pressure gradients.

We thank Professor P. K. Sen of the Indian Institute of Technology, Delhi for many interesting discussions and for generously sharing with us his eigenvalue solver for the Orr–Sommerfeld equation. We are grateful to Professor A. Prabhu (Indian Institute of Science) for useful discussions throughout the course of this project, Professor M. Gaster (Cambridge), Professor C. Grosch (Old Dominion University) and Dr T. K. Vashist (Bangalore) for their helpful comments on a preliminary account of this work, and Dr Sekhar Majumdar (National Aerospace Laboratories) for his continuous support. R.N. acknowledges a brief and fruitful visit to ICASE, NASA Langley in August 1993 that enabled useful discussions with Dr M. Y. Hussaini and his colleagues.

Appendix A. Comparison with existing formulations for Blasius flow

For Blasius flow, the present equation (11) is

$$\{\mathrm{OS}\}\phi+\frac{q}{R}\{a_3\mathrm{D}^3+a_2\mathrm{D}^2+a_1\mathrm{D}+a_0\}\phi+a_\alpha\alpha'\phi+a_\phi\frac{\partial\phi}{\partial x}=0. \tag{A 1}$$

Barry & Ross (1970) assumed a disturbance of the form

$$\hat{\phi}=\phi(y_d)\,\mathrm{e}^{\mathrm{i}[\alpha_d x_d-\omega_d t_d]},$$

where α_d is [locally] constant. The linearized two-dimensional Navier–Stokes equation, which we may write as

$$\{\mathscr{L}\}[\hat{\phi}_d]=0, \tag{A 2}$$

$$\{\mathscr{L}\}\equiv\frac{\partial}{\partial t_d}\nabla_d^2+\frac{\partial\Phi_d}{\partial y_d}\frac{\partial}{\partial x_d}\nabla_d^2+\frac{\partial}{\partial x_d}\nabla_d^2\Phi_d\frac{\partial}{\partial y_d}-\frac{\partial\Phi_d}{\partial x_d}\frac{\partial}{\partial y_d}\nabla_d^2-\frac{\partial}{\partial y_d}\nabla_d^2\Phi_d\frac{\partial}{\partial x_d}-\nu\nabla_d^4,$$

then reduces to

$$\left\{(\alpha U-\omega)(\mathrm{D}^2-\alpha^2)-\alpha\frac{\partial^2U}{\partial y^2}+\frac{\mathrm{i}}{R_0}(\mathrm{D}^2-\alpha^2)^2-\mathrm{i}V\mathrm{D}(\mathrm{D}^2-\alpha^2)+\mathrm{i}\frac{\partial^2V}{\partial y^2}\mathrm{D}\right\}\phi=0. \tag{A 3}$$

R_0 in (A 3) is based on a given (constant) boundary-layer thickness. The last two terms on the left-hand side of (A 3) account for the normal component of the mean velocity.

Substituting for V from the similarity streamfunction Φ, equation (A 3) may be written for Blasius flow as

$$\{\mathrm{OS}\}\,\phi+\frac{q}{R}\{(a_3-y\Phi')\,\mathrm{D}^3+[a_1+y(-2\omega\alpha+3\alpha^2\Phi'+\Phi''')]\,\mathrm{D}\}\,\phi=0. \tag{A 4}$$

Since this method does not account for all non-parallel effects, in particular for the x-dependence of the disturbance wavenumber and eigenfunction, (A 4) does not contain all the terms in (A 1).

Ling & Reynolds (1973) started with (A 2) non-dimensionalized by the free-stream velocity U_∞ and a length scale $(x_0\nu/U_\infty)^{1/2}$ where x_0 is constant. They wrote down expansions in a small parameter ϵ in the neighbourhood of a given point x_0 and obtained three equations which can be combined after neglecting higher-order terms in the mean flow to give

$$\{\mathrm{OS}\}\,\phi+a_\alpha\alpha'\phi+a_\phi\,\partial\phi/\partial x=0. \tag{A 5}$$

This equation omits the term containing the streamwise derivative of the length scale.

In their multiple-scale analysis, Saric & Nayfeh (1975) use the scale $x_1=\epsilon x$ to represent slow variations in x and derive two equations which, when combined putting $\epsilon=1/R$, give precisely the equation of Bertolotti *et al.*, which we now proceed to discuss.

In the present notation, the parabolic stability equation (6*a*) of Bertolotti *et al.* (1992) is given by

$$\{\mathrm{OS}\}\,\phi+\frac{q}{R}\{a_3\,\mathrm{D}^3+a_2\,\mathrm{D}^2+a_1\,\mathrm{D}+a_0\}\,\phi+a_\alpha\alpha'\phi+a_\phi\frac{\partial\phi}{\partial x}=\frac{a_R}{R^2}\phi, \tag{A 6}$$

$$a_R=2\mathrm{i}q\alpha[2y\mathrm{D}^3+3\mathrm{D}^2-2y\alpha^2\mathrm{D}-\alpha^2]-4\mathrm{i}\alpha(\mathrm{D}^2-\alpha^2)\,R\frac{\partial}{\partial x}-2\mathrm{i}R\alpha'(\mathrm{D}^2-3\alpha^2).$$

Equation (A 6) is the same as (A 1) except for the right-hand side, which contains certain $O(R^{-2})$ terms, indicating that the present formulation, in the special case of constant free-stream velocity, is consistent with that of Bertolotti *et al.* (1992) to $O(R^{-1})$; the inclusion of $O(R^{-2})$ terms would be unjustifiable unless the mean flow is known to the same order, which is hardly ever the case. Furthermore, it has been found that the right-hand side of (A 6) has no noticeable effect on the solution.

The expression used by Sen (1993) for the streamfunction is

$$\psi_d=U\delta^*\Phi+U\delta_0^*\,\phi(y)\,\mathrm{e}^{\mathrm{i}(\alpha x-\omega t)}. \tag{A 7}$$

On the assumption that δ_0^* is a constant, the following modified Orr–Sommerfeld equation is derived where δ_0^* has been taken to be numerically equal to δ^*:

$$\{\mathrm{OS}\}\,\phi+\frac{q}{R}\{a_3\,\mathrm{D}^3+2a_2\,\mathrm{D}^2+a_1\,\mathrm{D}\}\,\phi=0. \tag{A 8}$$

It is straightforward to show that the x-derivative of δ_0^* gives rise to the additional terms $q/R(-a_2\,\mathrm{D}^2+a_0)\,\phi$ in (A 1).

Appendix B. Free-stream boundary conditions

As the computations are carried out in a finite domain, it is important to derive the form of the (decaying) eigenfunction at large y to ensure that the correct free-stream boundary conditions are satisfied by the computed solution. At y much greater than

the boundary-layer thickness $\Phi' = 1$, $\Phi'' = \Phi''' = 0$ and $\Phi = y - \delta^*/\theta$ except for exponentially small terms in y, and the Orr–Sommerfeld equation (1) reduces to one with constant coefficients which has four solutions. Two of these are rejected because they indicate exponentially increasing disturbances at large y, which is unphysical, while the third is not considered since it decays much faster than the solution which is retained,

$$\phi \sim \mathrm{e}^{-\alpha y}. \tag{B 1}$$

In the non-parallel formulation (6), the coefficients of the first and third derivatives in y of ϕ as well as the right-hand side are functions of y outside the boundary layer; for y_a much greater than the boundary-layer thickness δ, equation (6) reduces to

$$\begin{aligned}\frac{1}{R}\Big\{\mathrm{D}^4 + p\left(y - \frac{\delta^*}{\theta}\right)\mathrm{D}^3 + [\mathrm{i}R(\omega-\alpha) - 2\alpha^2 + 2q - p]\,\mathrm{D}^2 \\ + [2yq\alpha(\omega-\alpha) - p\alpha^2(y-\delta^*/\theta)]\,\mathrm{D} + [\alpha^4 - \mathrm{i}R\alpha^2(\omega-\alpha) + (q-2p)\,\alpha\omega \\ + 3(p-q)\,\alpha^2 - (\omega-3\alpha)\,R\alpha'] + [3\alpha^2 - 2\alpha\omega - \mathrm{D}^2]\,R\,\partial/\partial x\Big\}\phi = 0.\end{aligned} \tag{B 2}$$

Since this equation has additional terms of order R^{-1} compared to the Orr–Sommerfeld equation, it is reasonable to expect that the behaviour in the far field will be modified by effects of this order. Therefore the form for the decay of the disturbance streamfunction outside the boundary layer will differ from (B 1), and may be assumed to be

$$\phi = h(x)\,\mathrm{e}^{g(x,y) - \alpha(x)y}, \tag{B 3}$$

where $h'(x)$ and g are both $O(R^{-1})$. When (B 3) is substituted into (B 2) one obtains a second-order linear differential equation for g,

$$\mathrm{D}^2 g - 2\alpha \mathrm{D}g + [t_1 - 2\alpha t_2 - 2y\alpha t_1] = 0, \tag{B 4}$$

where

$$t_1 = (q\alpha - R\alpha')/\mathrm{i}R, \quad t_2 = (p + R(h'/h))/\mathrm{i}R.$$

The solution is

$$g = -\tfrac{1}{2}t_1 y^2 - t_2 y + \frac{1}{2\alpha}\left[\left(\frac{1}{2\alpha}+1\right)t_1 - t_2\right] + c_1\,\mathrm{e}^{2\alpha y} + c_2. \tag{B 5}$$

The constant c_1 is set equal to 0 on the grounds that ϕ must decay at large y. Equation (B 3) then gives

$$\phi = c_2 h(x) \exp\left[\left(\frac{1}{2\alpha}+1\right)\frac{t_1}{2\alpha} - \frac{t_2}{2\alpha}\right] \exp\left[-\alpha y - t_2 y - \tfrac{1}{2}t_1 y^2\right]. \tag{B 6}$$

Now putting

$$f(x) = c_2 h(x) \exp\left[\left(\frac{1}{2\alpha}+1\right)\frac{t_1}{2\alpha} - \frac{t_2}{2\alpha}\right],$$

and noting that t_1 and t_2 are both $O(R^{-1})$, we have

$$\frac{f'}{f} = \frac{h'}{h} + O\left(\frac{1}{R^2}\right).$$

Equation (B 6) may therefore be written as

$$\phi = f(x) \exp\left[-\alpha y + \mathrm{i}\frac{p + Rf'/f}{R}y + \mathrm{i}\frac{q\alpha - R\alpha'}{2R}y^2\right], \tag{B 7}$$

which is the required boundary condition as $y \to \infty$.

Appendix C. Higher-order mean flow

Taking account of higher-order effects, the free-stream velocity U over a boundary layer may be expanded as

$$U(x_d) = U_0(x_d) + \epsilon U_1(x_d) + o(\epsilon), \tag{C 1}$$

where ϵ is a constant of $O(R^{-1})$. For the flow over a semi-infinite wedge,

$$U_0 = Bx_d^m, \tag{C 2}$$

where B and m are constants. The higher-order mean flow arising owing to the displacement thickness may be derived from the potential flow theory of the flow over thin airfoils (Van Dyke 1975),

$$\epsilon U_1 = \frac{1}{\pi}\int_0^\infty \frac{U_0(\xi)}{(x_d-\xi)}\frac{\mathrm{d}\delta_0^*}{\mathrm{d}x_d}(\xi)\,\mathrm{d}\xi, \tag{C 3}$$

where δ_0^* is the lowest-order displacement thickness. The integral in (C 3) has the form of a Hilbert transform, which can be evaluated to give

$$\epsilon U_1 = \frac{U_0 Hq}{R\tan(\frac{1}{2}(m+1)\pi)} = \frac{CU_0}{R}, \tag{C 4}$$

where H is the shape factor which is constant for a given Falkner–Skan profile. The higher-order velocity profile is derived from the equations (Van Dyke 1962)

$$\frac{\partial u_1}{\partial x_d}+\frac{\partial v_1}{\partial y_d} = 0, \tag{C 5}$$

$$u_0\frac{\partial u_1}{\partial x_d}+u_1\frac{\partial u_0}{\partial x_d}+v_0\frac{\partial u_1}{\partial y_d}+v_1\frac{\partial u_0}{\partial y_d}-\nu\frac{\partial^2 u_1}{\partial y_d^2}-\frac{d(U_0U_1)}{dx_d} = 0, \tag{C 6}$$

where u_0 and v_0 are the lowest-order velocity components in the streamwise and normal directions respectively while u_1 and v_1 are the corresponding first-order components such that

$$u_d = u_0+\epsilon u_1+o(\epsilon) \quad \text{and} \quad v_d = v_0+\epsilon v_1+o(\epsilon).$$

We look for a similarity solution for u_1 of the form

$$u_1 = G(x_d)\,\Phi_1'(\eta), \quad \eta = y_d/(x_d)^b \tag{C 7}$$

where b is a similarity exponent which is obtained below. The last term in (C 6) is found using equations (C 2) and (C 4), and u_0 and v_0 are known from the Falkner–Skan solution. Using (C 5) and (C 7) to express v_1 in terms of G and Φ_1, (C 6) reduces to

$$\Phi_1'''+\frac{x_d^b}{\nu}[(\theta U_0)'\,\Phi_0+U_0(b\eta x_d^{b-1}-\theta' y)\,\Phi_0']\,\Phi_1''-\frac{x_d^{2b}}{\nu}\left[\left(U_0\frac{G'}{G}+U_0'\right)\Phi_0'\right.$$

$$\left.+\left(\frac{U_0}{\theta}\right)(b\eta x_d^{b-1}-\theta' y)\,\Phi_0''\right]\Phi_1'+\frac{x_d^{3b}\,U_0\,\Phi_0''}{\theta\nu}\left[\frac{G'}{G}+\frac{b}{x_d}\right]\Phi_1+\frac{CU_0\,x_d^{2b-1}(3m-1)}{2\theta G\epsilon} = 0. \tag{C 8}$$

It is to be kept in mind that the primes on Φ_0 refer to differentiation with respect to y while those on Φ_1 refer to differentiation with respect to η. For a similar solution, the coefficients of (C 8) must be independent of the streamwise location. Applying this

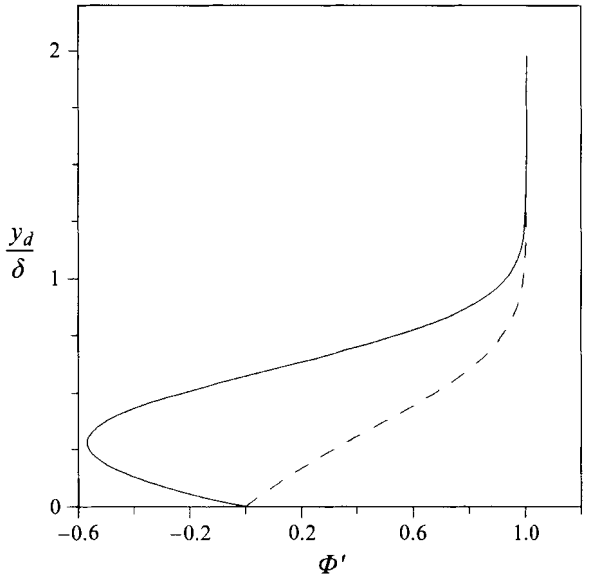

FIGURE 16. Mean velocity profiles for $m = -0.06$. --, Falkner–Skan, Φ_0'; —, solution for displacement-effect correction, Φ_1'.

condition to the coefficient of the second derivative Φ_1'', we get $b = (1-m)/2$, which means that η is actually proportional to y:

$$\eta = \left(\frac{2q\nu}{B(1-m)}\right)^{1/2} y;$$

thus the first-order mean flow obeys the same similarity as the zeroth-order flow. We now choose

$$G'/G = -b/x_d \quad \text{or} \quad G = Dx_d^{(m-1/2)},$$

with D independent of x_d, which makes the coefficient of Φ_1 in (C 8) equal to zero. With these substitutions (C 8) becomes the ordinary differential equation

$$\Phi_1''' + \frac{1+m}{2}\left(\frac{2qB}{(1-m)\nu}\right)^{1/2}\Phi_0\Phi_1'' + \frac{B}{2\nu}(1-3m)\left(\Phi_0'\Phi_1' - \frac{C}{\epsilon D}\left(\frac{B\nu(1-m)}{2q}\right)^{1/2}\right) = 0. \quad \text{(C 9)}$$

Since G may be multiplied by any factor independent of x_d if the far-field conditions are suitably adjusted, D may be chosen as

$$D = \frac{C}{\epsilon}\left(\frac{B\nu(1-m)}{2q}\right)^{1/2} \quad \text{giving} \quad G = U_1.$$

The order of (C 9) may be reduced by one by putting $z = \Phi_1'$, and the independent variable changed to y for uniformity to give

$$z'' + p\Phi_0 z' + (2q-p)[\Phi_0' z - 1] = 0. \quad \text{(C 10)}$$

The mean dimensional velocity and streamfunction are thus given by

$$u_d = U_0\left(\Phi_0' + \frac{C}{R}\Phi_1'\right) \quad \text{and} \quad \Phi_d = U_0\theta\left(\Phi_0 + \frac{C}{R}\Phi_1\right). \quad \text{(C 11)}$$

A sample result for the higher-order velocity profile is shown in figure 16.

REFERENCES

BARRY, M. D. J. & ROSS, J. A. 1970 The flat plate boundary layer. Part 2. The effect of increasing thickness on stability. *J. Fluid Mech.* **43**, 813–818.

BERTOLOTTI, F. P. 1991 Linear and nonlinear stability of boundary layers with streamwise varying properties. PhD thesis, Ohio State University.

BERTOLOTTI, F. P., HERBERT, TH. & SPALART, P. R. 1992 Linear and nonlinear stability of the Blasius boundary layer. *J. Fluid Mech.* **242**, 441–474.

BOUTHIER, M. 1972 Stabilite lineaire des ecoulements presque paralleles. Part I. *J. Méc.* **11**, 599–621.

BOUTHIER, M. 1973 Stabilite lineaire des ecoulements presque paralleles. Part II, La couche limite de Blasius. *J. Méc.* **12**, 75–95.

CEBECI, T. & SMITH, A. M. O. 1974 *Analysis of Turbulent Boundary Layers*. Academic.

DEY, J. & NARASIMHA, R. 1990 An extension of the Thwaites method for calculation of incompressible laminar boundary layers. *J. Indian Inst. Sci.* **70**, 1–11.

DRAZIN, P. G. & REID, W. H. 1981 *Hydrodynamic Stability*. Cambridge University Press.

FASEL, H. F. & KONZELMANN, U. 1990 Non-parallel stability of a flat plate boundary layer using the complete Navier–Stokes equations. *J. Fluid Mech.* **221**, 311–347.

GASTER, M. 1974 On the effects of boundary layer growth on flow stability. *J. Fluid Mech.* **66**, 465–480.

GOVINDARAJAN, R. 1994 Stability of spatially developing boundary layers in pressure gradients. PhD thesis, Indian Institute of Science.

GRAEBEL, W. P. 1966 On determination of the characteristic equations for the stability of parallel flows. *J. Fluid Mech.* **24**, 497–508.

HORSTMANN, K. H., QUAST, A. & REDEKAR, G. 1990 Flight and wind tunnel investigations on boundary layer transition. *J. Aircraft* **27**, 146–150.

KLINGMANN, B. G. B., BOIKO, A. V., WESTIN, K. J. A., KOZLOV, V. V. & ALFREDSSON, P. H. 1993 Experiments on the stability of Tollmien–Schlichting waves. *Eur. J. Mech.* B *Fluids* **12**, 493–514.

LING, C.-H. & REYNOLDS, W. C. 1973 Non-parallel flow corrections for the stability of shear flows. *J. Fluid Mech.* **59**, 571–591.

MILEY, S. J. 1982 A catalogue of low Reynolds number airfoil data for wind tunnel applications. Dept. of Aerosp. Eng., Texas A & M University.

ROSS, J. A., BARNES, F. H., BURNS, J. C. & ROSS, M. A. 1970 The flat plate boundary layer. Part 3. Comparison of theory with experiments. *J. Fluid Mech.* **43**, 819–832.

SARIC, W. S. 1990 Low speed experiments: requirements for stability measurements. In *Instability and Transition* (ed. M. Y. Hussaini & R. G. Voigt). Springer.

SARIC, W. S. & NAYFEH, A. H. 1975 Nonparallel stability of boundary layer flows. *Phys. Fluids* **18**, 945–950.

SCHUBAUER, G. B. & SKRAMSTAD, H. K. 1948 Laminar boundary layer oscillations and transition on a flat plate. *NACA Rep.* 909.

SEN, P. K. 1993 Some recent developments in the theory of boundary layer instability. *Sādhanā* **18**, 387–403.

SMITH, A. M. O. & GAMBERONI, N. 1956 Transition, pressure gradient and stability theory. *Douglas Aircraft Company Rep.* ES26388.

SMITH, F. T. 1979 On the non-parallel flow stability of the Blasius boundary layer. *Proc. R. Soc. Lond.* A **366**, 91–109.

THWAITES, B. 1949 Approximate calculation of the laminar boundary layer. *Aero. Q.* **1**, 245–280.

VAN DYKE, M. 1962 Higher approximations in boundary-layer theory. Part 1. General analysis. *J. Fluid Mech.* **14**, 161–177.

VAN DYKE, M. 1975 *Perturbation Methods in Fluid Mechanics*. Parabolic.

VAN INGEN, J. L. 1956 A suggested semi-empirical method for the calculation of the boundary layer transition region. *Delft University of Technology, Dept. of Aero. Engng Rep.* UTH-74.

VIKEN, J. K. 1986 Boundary layer stability and airfoil design. *NASA CP* 2413.

WAZZAN, A. R., TAGHAVI, H. & KELTNER, G. 1974 Effect of boundary layer growth on stability of incompressible flat plate boundary layer with pressure gradient. *Phys. Fluids* **17**, 1655–1660.